

# Lattice QCD and Three-particle Decays of Resonances

Maxwell T. Hansen,<sup>1</sup> and Stephen R. Sharpe<sup>2</sup>

<sup>1</sup>Theoretical Physics Department, CERN, 1211 Geneva 23, Switzerland; email: maxwell.hansen@cern.ch

<sup>2</sup>Physics Department, University of Washington, Seattle, WA 98195, USA; email: srsharpe@uw.edu

Xxxx. Xxx. Xxx. Xxx. YYYY. AA:1–31

[https://doi.org/10.1146/\(\(please add article doi\)\)](https://doi.org/10.1146/((please add article doi)))

Copyright © YYYY by Annual Reviews.  
All rights reserved

## Keywords

finite-volume quantum field theory, lattice QCD, three-particle quantization condition, resonances

## Abstract

Most strong-interaction resonances have decay channels involving three or more particles, including many of the recently discovered  $X$ ,  $Y$  and  $Z$  resonances. In order to study such resonances from first principles using lattice QCD, one must understand finite-volume effects for three particles in the cubic box used in calculations. Here we review efforts to develop a three-particle quantization condition that relates finite-volume energies to infinite-volume scattering amplitudes. We describe in detail the three approaches that have been followed, and present new results on the relationship between the corresponding results. We show examples of the numerical implementation of all three approaches and point out the important issues that remain to be resolved.

## Contents

1. INTRODUCTION .....	2
2. RELATIVISTIC QUANTIZATION CONDITIONS USING A DIAGRAMMATIC APPROACH IN QFT .....	5
2.1. Two-particle quantization condition in the RFT approach .....	5
2.2. Three-particle quantization condition in the RFT approach .....	9
2.3. Truncating the quantization condition .....	15
2.4. Analytic investigations of the RFT quantization condition .....	15
3. ALTERNATIVE APPROACHES .....	16
3.1. NREFT approach .....	17
3.2. Finite-volume unitarity (FVU) approach .....	22
4. NUMERICAL IMPLEMENTATIONS .....	26

## 1. INTRODUCTION

One of the striking features of the strong interaction is the abundance of resonances. These are very short-lived (having widths  $\Gamma \sim 100$  MeV), and are not asymptotic states, but are manifested through the behavior of the scattering amplitudes of particles that are stable under the strong interactions, e.g. pions, kaons and nucleons. Examples of resonances include the rho, decaying via  $\rho \rightarrow \pi\pi$ , as well as the  $a_1(1260) \rightarrow \pi\pi\pi$  and the Roper resonance,  $N(1440) \rightarrow N\pi, N\pi\pi$ , where in each case we have shown the final states with the highest branching fractions.

The lightest such resonances form patterns when arranged according to basic properties such as spin, charge and strangeness, for example the flavor SU(3) decuplet of  $J = 3/2$  baryons ( $\Delta$ ,  $\Sigma^*$ ,  $\Xi^*$ , and  $\Omega$ ) and the nonet of  $J^P = 1^-$  mesons ( $\rho$ ,  $\omega$ ,  $K^*$ , and  $\phi$ ). This regularity, together with that of the particles stable under strong decay, was crucial in determining the underlying degrees of freedom, the quarks and gluons. This culminated in the formulation of quantum chromodynamics (QCD) in the early 1970s (1, 2, 3).

While the lightest resonances can be categorized in quark-model language as quark-antiquark and three-quark states, this does not hold for higher-lying states. Examples include the  $f_0(980)$  and  $a_0(980)$ , long considered to have a tetraquark ( $qq\bar{q}\bar{q}$ ) component (4), and pentaquark candidates such as the  $P_c(4450)^+$  (5). Other resonances that do not fit into the simple quark-model classification are the recently discovered  $X$ ,  $Y$  and  $Z$  states, which contain open or hidden charm and bottom quarks. For a recent summary of the experimental and theoretical status of the many states whose classification is unclear, see Ref. (6) and the Particle Data Group listings and reviews (7).

This situation, and in particular the multitude of  $X$ ,  $Y$  and  $Z$  resonances, has led to a resurgence of interest in hadron spectroscopy, and a renewed appreciation of the need to extract predictions from first-principles QCD. In particular, many of the new states lie close to thresholds, and involve decays to multiple channels, and it is crucial to disentangle kinematical effects such as threshold cusps from truly resonant behavior. The latter is identified as a pole in the analytic continuation of a scattering amplitude to complex values of the center-of-mass energy.

A crucial tool in disentangling the underlying properties of such resonances is first-principles calculations based in lattice QCD (LQCD). With this method, unlike with the quark model or other approximate approaches, one can systematically remove all sources of uncertainty in the calculations. The major such sources are the statistical errors inherent in a Monte Carlo calculation, the need to work at nonzero lattice spacing, the use of larger-than-physical quark masses, and the need to work with a finite space-time volume, with spatial box length<sup>1</sup>  $L$  and Euclidean time extent  $L_t$ . Over the last decade or so, an increasing number of LQCD results for single-particle quantities have controlled all of these errors, in some cases at subpercent precision. One indication of this improved level of control is the increasingly common use of physical light-quark masses in calculations. For a review of results for well-controlled single-particle quantities using LQCD, see Ref. (8).

Using LQCD to calculate the properties of resonances is, however, more challenging than for single-particle properties. A resonance is observed experimentally by studying the scattering of the decay products, e.g. two pions in the case of the  $\rho$  resonance. By measuring scattering rates for various kinematics and then performing a partial-wave analysis, one can in principle determine the scattering amplitudes projected to any given angular-momentum component and search for resonances. Lattice calculations cannot, however, reproduce this setup. The use of a finite volume does not allow the consideration of states with well-separated decay products (so one cannot approach the in- and out-states needed for a theoretical description of scattering in quantum field theory) and the need to use Euclidean time (in order to avoid a numerically intractable sign problem) makes real-time processes such as scattering inaccessible. Thus one is forced to use an indirect approach.

The indirect approach that is by now widely applied was first introduced in seminal work by Lüscher (9, 10, 11). The essential observation is that the volume dependence of the energies of

<sup>1</sup>Most LQCD calculations use cubic spatial boxes, and we consider only this case in this review.

multiparticle states is governed by infinite-volume scattering amplitudes. By determining, in a lattice calculation, the finite-volume spectrum as a function of  $L$ , one is thus doing something analogous to a scattering experiment. Crudely speaking, the multi-particle finite-volume state in a large enough box contains particles that are almost moving freely, and thus approximate a scattering state.

In the case of resonances that only decay to channels containing two particles, this has been placed on a rigorous footing by the derivation of so-called two-particle quantization conditions, i.e. equations that are satisfied only at the energies of finite-volume states and yet depend on infinite-volume scattering quantities. The simplest cases were worked out in Refs. (9, 10, 11) (and will be reviewed in subsequent sections), and extensions to arbitrary spins, noncubic boxes, moving frames, and multiple two-particle channels have been subsequently derived. We do not review this literature here, as it is not the topic of this work, but point the interested reader to the comprehensive review provided in Ref. (12).

We now come to the essential phenomenological motivation for the present review: Most resonances have some decay channels that involve three or more stable hadrons. Examples noted above are the  $a_1(1260)$ , with a dominant decay into three pions, the Roper resonance, which decays both to two- and three-particle channels, and many of the  $X$ ,  $Y$  and  $Z$  resonances. For such resonances, the two-particle formalism simply does not apply. Thus, in order to address many pressing questions in hadron spectroscopy using LQCD, a three-particle quantization condition is needed. This is an equation that, given information about two- and three-particle scattering, predicts the finite-volume spectrum or, conversely, provides constraints on the scattering amplitudes given the spectrum calculated using LQCD.<sup>2</sup> The major purpose of this review is to explain the theoretical progress that has been made over the last five or so years in deriving three-particle quantization conditions.

Another motivation for this review is that advances in algorithms, methods, and the speed of computers, have allowed LQCD calculations to determine the finite-volume spectrum in the energy regime in which states have a significant three-particle component. Many examples can be found in Ref. (12), but we note in particular the spectra determined in Refs. (13) and (14). At present, these calculations use heavier-than-physical quarks (so that  $m_\pi \gtrsim 230$  MeV), but, nevertheless, their interpretation requires a quantization condition that can account for three, and in some cases more, particles. Indeed, the need for such a quantization condition becomes more pressing as the quark masses are lowered to their physical values, for then the multi-pion thresholds drop rapidly.

Although motivated by results from LQCD, the derivations of the quantization conditions are in fact based in finite-volume continuum quantum field theory (QFT). In particular, we assume in the following that calculations have controlled the errors associated with nonzero lattice spacing and unphysical quark masses by appropriate extrapolations (or, in the latter case, possibly interpolations). As noted above, there are also errors associated with the finite extent of the lattice in the Euclidean time direction,  $L_t$ . Lattice calculations are mostly done with boundary conditions in the temporal direction chosen to give the system a thermal interpretation, with temperature  $T = 1/L_t$ . By choosing  $L_t$  large enough one works at very low temperatures, and then it is possible to extract the spectrum with controlled errors from the dependence of correlators on the Euclidean time separation. Thus the only issue we address here is the impact of working in a finite, cubic box, of length  $L$ . We further assume that, as in most lattice calculations, the spatial boundary conditions are periodic.

Within this box one can fix all internal quantum numbers of the overall state. For example, one can set  $Q = |e|$ ,  $B = S = 0$  ( $B$  being baryon number, and  $S$  strangeness), choose odd G-parity,<sup>3</sup> and also fix the total three-momentum  $\vec{P}$  to one of the allowed finite-volume values  $2\pi\vec{n}/L$  (with  $\vec{n}$  a vector of integers). Then the lightest finite-volume state corresponds to a  $\pi^+$  with momentum  $\vec{P}$ , and the excitations correspond to interacting  $\pi^+\pi^+\pi^-$  and  $\pi^+\pi^0\pi^0$  states. If instead one projects onto  $Q = 2|e|$  and even G-parity, while keeping  $B = S = 0$ , then the available states are approximately described as interacting  $\pi^+\pi^+$ ,  $\pi^+\pi^+\pi^+\pi^-$  and  $\pi^+\pi^+\pi^0\pi^0$  states, etc. Similarly, if we take  $Q = 3|e|$  and odd G-parity, then the lightest state consists of  $\pi^+\pi^+\pi^+$ .

It is important to keep in mind, however, that we do not need to keep track of the individual particle components. We simply create the state with an operator having the requisite quantum numbers. Then the QCD dynamics, encoded in terms of quarks and gluons interacting via the QCD Lagrangian, lead to a low-lying spectrum of multi-hadron finite-volume states. The only output is a set of  $L$ -dependent energy levels, and this is all the input needed by the quantization conditions.

It will be useful for the more technical discussion of the subsequent sections to describe some general features of the dependence of energy levels on  $L$ . For single, stable particles, a key result is that the energies, and other properties, depend on volume as  $(M_\pi L)^{-n} \exp(-\alpha M_\pi L)$ , where  $n$  and  $\alpha$  depend on the quantity (9). These corrections arise from virtual pions propagating to the

---

**Lüscher's method::**  
Determine resonance properties from finite-volume spectrum

---



---

**Box length,  $L$ :**  
Periodicity of the finite-volume in each of the three spatial directions

---

<sup>2</sup>As we will see in subsequent sections, the connection between finite-volume spectrum and scattering amplitudes is more indirect in the three-particle case compared to that for two particles.

<sup>3</sup>To keep the examples discussed in this paragraph simple, we work in the limit of exact isospin symmetry.

---

**Key approximation::**  
Neglect of  
exponentially-  
suppressed volume  
dependence

---

neighboring cells of the periodic system. They drop off rapidly with  $L$ , and it has been found that using  $M_\pi L \gtrsim 4$  is usually sufficient for finite-volume uncertainties to become subleading to other sources. Throughout this review, we assume that such exponentially-suppressed dependence can be neglected. The weakness of such dependence is crucial for the above-described successes of LQCD in attaining subpercent precision for certain single-particle quantities.

The volume dependence for multiple-particle states is, however, quite different. In this case the asymptotic behavior exhibits power-law scaling of the form  $L^{-n}$ . We describe the origin of this behavior below, but for now note only that multiparticle finite- $L$  effects fall off much more slowly than the exponentially suppressed terms and cannot be ignored. Indeed, the quantization conditions allow this dependence to be used as a tool rather than an unwanted artifact. In this way, an apparent source of systematic uncertainty in LQCD calculations has become a powerful window into resonance physics.

This review is organized as follows. Three approaches have been followed in the development of the three-particle quantization condition, and we discuss them in turn.<sup>4</sup> The first uses a diagrammatic, all-orders analysis in a generic effective QFT. We refer to this as the RFT approach, with the R emphasizing that this is a relativistic approach. It was developed by us in Refs. (17, 18) for the simplest case of three identical scalars with a  $Z_2$  symmetry forbidding  $2 \leftrightarrow 3$  transitions, and subsequently generalized in collaboration with Briceño in Refs. (19, 20). This is the topic of the following section, Sec. 2. We first describe the derivation of the two-particle quantization condition in Sec. 2.1, providing two simple examples in order to motivate the general derivation. We then, in Sec. 2.2, provide a description of the derivation of the three-particle quantization condition. Here we are able to use results from Ref. (20) to simplify and shorten the derivation given in the original work, Ref. (17). Our hope is that this will make this rather technical derivation more accessible. We close Sec. 2 with brief discussions of how the three-particle quantization condition can be truncated and thus made practical, and of two analytic checks of the formalism.

Two alternate approaches have subsequently been followed, both of which greatly simplify the derivation of the quantization condition. These are described in Sec. 3. To date, these only consider the case in which the interaction between particle pairs (denoted “dimers”) is purely  $s$ -wave. This is in contrast to the RFT approach, for which all waves are included in the dimer interactions. The two alternate approaches are that based on non-relativistic effective field theory (NREFT) (21, 22), and that using a finite-volume implementation of unitarity constraints, which we refer to as the finite-volume unitarity (FVU) approach (23, 24). For both approaches we describe the derivation of first the two- and then the three-particle quantization conditions, and then describe the relation of the results to those in the RFT approach. These latter two sections, Secs. 3.1.3 and 3.2.3, present new results, which we think illuminate the similarities and differences between the approaches.

A key question for all approaches is whether they can be implemented in practice. This has been addressed over the last year or so in all three approaches by showing how, in the simplest approximation of  $s$ -wave dimer interactions and a local three-particle interaction, the quantization conditions can be used to predict the finite-volume spectrum. Sec. 4 gives examples of the results from all three approaches.

We close with a list of summary points and issues for future work.

In order to keep this review within bounds, there are many topics that we do not cover. As already noted, we do not discuss, except in passing, the two-particle formalism, or the extensive numerical results from LQCD calculations using the two-particle quantization condition to determine two-particle scattering amplitudes. For a recent, thorough review of both of these topics, we refer the reader again to Ref. (12).

We also do not discuss the approach to two- and three-particle systems developed by the HALQCD collaboration, and reviewed in Ref. (25). In the two-particle case, this approach uses the Bethe-Salpeter amplitude in order to extract a potential that can then be inserted into the Schrödinger equation to determine bound-state energies and scattering amplitudes. It has been successfully applied to many two-baryon systems—for a recent example see Ref. (26). The extension to three particles (27) is, however, so far restricted to the nonrelativistic domain, and thus is not directly applicable to most of the resonances of interest in QCD.

We also do not discuss the impressive recent progress in simulating multiple interacting nucleons by discretizing the truncated pionless chiral EFT, and working in a finite volume. For a review see Ref. (28), and for an example of recent work see Ref. (29). This is a powerful method for studying bound states and near-threshold behavior, but does not apply to the resonances of interest, where dynamical pions are essential.

Finally, we do not discuss recent ideas for determining the finite-volume multi-particle spectrum in NRQM using a variational approach (30), as again this is restricted to the nonrelativistic regime.

---

<sup>4</sup>We also note the pioneering work of Ref. (15), which showed that the three-particle spectrum depends only on S-matrix elements. Another early step towards a quantization condition was taken in Ref. (16).

## 2. RELATIVISTIC QUANTIZATION CONDITIONS USING A DIAGRAMMATIC APPROACH IN QFT

In this section we review the derivations of the two- and three-particle quantization conditions using an all-orders diagrammatic analysis in a generic relativistic field theory. We refer to this as the RFT approach. We begin with two particles as this allows us to explain the general strategy and to introduce notation that will aid in the explication of the more complicated case of three particles. We will derive these results in the simplest setting, namely for identical, spinless particles, which is the only setting considered to date for the three-particle quantization condition.

### 2.1. Two-particle quantization condition in the RFT approach

The two-particle quantization condition provides the relation between the spectrum of a field theory in a finite box and the infinite-volume two-to-two scattering amplitude,  $\mathcal{M}_2$ . We begin with some kinematical notation for  $\mathcal{M}_2$ . We use  $P^\mu = (E, \vec{P})$  to denote the total 4-momentum of the scattering pair, so that  $P^\mu P_\mu = E^2 - \vec{P}^2 = s$ . Denoting the 4-momentum of one of the incoming particles as  $k$ , and that of one of the outgoing as  $k'$ , we write the dependence of the amplitude as  $\mathcal{M}_2(P; k', k)$ . We use this notation also for off-shell amplitudes, for which  $k^\mu k_\mu \neq m^2$ , with  $m$  the physical mass of the particle.<sup>5</sup> A special role is played by the c.m. (center-of-momentum) frame. We denote quantities in this frame with a superscript  $*$ , e.g. the total energy is  $E^* = \sqrt{s}$ , and the incoming 3-momentum  $\vec{k}$  boosted to this frame is  $\vec{k}^*$ . When the two incoming particles, with momenta  $k$  and  $P - k$ , are each on shell, this implies a constraint on the magnitude of the CM-frame momentum,  $k^* \equiv |\vec{k}^*|$ . In this case one finds that the latter is equal to  $q^* = \sqrt{E^{*2}/4 - m^2}$ , meaning that for fixed  $E^*$  only angular degrees of freedom remain. This allows one to decompose the on-shell amplitude into angular-momentum components,  $\mathcal{M}_2^{(\ell)}(s)$ , in the standard way.

Unitarity provides an important constraint on  $\mathcal{M}_2^{(\ell)}(s)$ , one that will play a central role in Sec. 3.2.1. Specifically, it implies that, for  $s \geq 4m^2$ ,

$$\mathcal{M}_2^{(\ell)}(s)^{-1} = \mathcal{K}_2^{(\ell)}(s)^{-1} - i\rho(s), \quad \mathcal{K}_2^{(\ell)}(s)^{-1} = \frac{q^* \cot \delta^{(\ell)}(q^*)}{16\pi\sqrt{s}}, \quad \rho(s) = \frac{q^*}{16\pi\sqrt{s}}, \quad (1)$$

where the K matrix,  $\mathcal{K}_2^{(\ell)}(s)$ , is a real function that is meromorphic (analytic up to poles) for  $s > 0$ . When we discuss the three-particle case we need to consider  $\mathcal{M}_2^{(\ell)}(s)$  below threshold such that  $q^{*2} < 0$ . To make sense of this is useful to note that  $\mathcal{M}_2^{(\ell)}(s)$  has a branch cut along the real axis in the complex  $s$  plane, running from  $s = 4m^2$  to  $\infty$ . The conventions established above correspond to real energies just above the cut. To remain on the same Riemann sheet for  $s < 4m^2$ , one must analytically continue the phase-space factor as  $\rho(s) = i|q^*|/(16\pi\sqrt{s})$ .

Turning now to the finite volume, we open with only a brief comment on our set up: In this review we restrict attention to periodic, cubic volumes, with length  $L$  in each of the three spatial directions.

**2.1.1. Example: leading term in the threshold expansion.** To gain intuition into the general approach, we discuss two simple examples of the derivation of the quantization condition. The first concerns the lowest two-particle energy for  $\vec{P} = 0$ , which, as was already shown over 60 years ago (32), satisfies

$$E_0(L) = 2m + 4\pi a/(mL^3) + \mathcal{O}(1/L^4). \quad (2)$$

Here  $a$  is the scattering length, defined by

$$q^* \cot \delta^0(q^*) = -1/a + \mathcal{O}(q^{*2}). \quad (3)$$

It is convenient here, and in the following, to introduce a finite-volume correlator that is closely related to the two-to-two scattering amplitude,  $\mathcal{M}_2$ . This object, called  $\mathcal{M}_{2L}$ , will have poles at the energies of the finite-volume states. It is defined by calculating exactly the same set of Feynman diagrams as for  $\mathcal{M}_2$ , but with a sum rather than an integral over the allowed three-dimensional momentum modes. For example, in  $\lambda\phi^4$  theory, the leading-order and next-to-leading-order contributions are shown in **Figure 1(a)** and given by

$$i\mathcal{M}_{2L} \equiv -i\lambda - \frac{\lambda^2}{2} \int \frac{d\ell^0}{2\pi} \frac{1}{L^3} \sum_{\vec{\ell}} \frac{i}{\ell^2 - m^2 + i\epsilon} \frac{i}{(P - \ell)^2 - m^2 + i\epsilon} + \dots + \mathcal{O}(\lambda^3), \quad (4)$$

where the ellipses represents the  $t$ - and  $u$ -channel diagrams. Some choice of UV regularization is implicit here, but need not be specified as it will play no role in the final result.

Our aim is now to pull out the power-law volume dependence. If all sums were replaced by integrals, then we would simply obtain the second-order expression for  $\mathcal{M}_2$ . For the  $t$ - and  $u$ -

<sup>5</sup>These are defined as the sum of all two-to-two amputated diagrams using the fundamental field of the theory as the external operator. Field redefinitions can change these amplitudes off shell, but the on-shell values, which are all that enter our final expressions, are invariant.

---

**Superscript \*:**  
Denotes quantities defined in the c.m. frame.

---



---

$\mathcal{K}_2^{(\ell)}(s)$ : Relation between K matrix and scattering amplitude

---



---

**Threshold expansion:**  
Leading order term

---

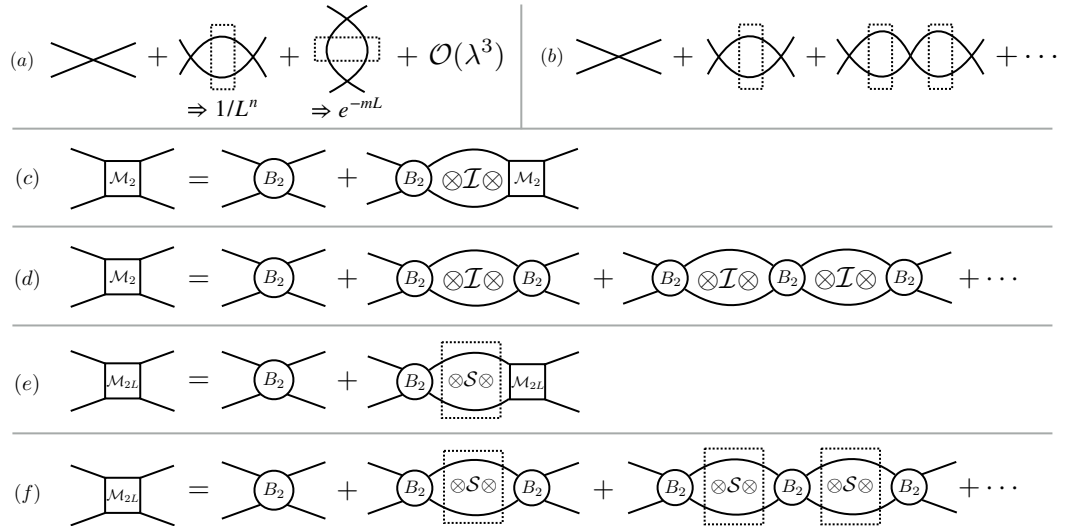


**Figure 1**

Representations of the scattering amplitude,  $\mathcal{M}_2$  and its finite-volume correspondent,  $\mathcal{M}_{2L}$ . (a) First- and second-order contributions to  $\mathcal{M}_{2L}$  in  $\lambda\phi^4$  theory, with the dashed rectangles indicating that the spatial momenta are summed over the discrete finite-volume values. (b) The set of diagrams that must be summed in order to calculate the leading order energy shift in  $\lambda\phi^4$  theory. (c) Bethe-Salpeter (BS) equation for the infinite-volume amplitude, with  $B_2$  being the BS kernel. (d) Iterated version of the BS equation. (e) BS equation for the finite-volume amplitude, with  $\mathcal{S}$  and the dashed rectangle both indicating a sum over finite-volume three-momenta. (f) Iterated version of finite-volume BS equation.

channel contributions, it can be shown, as discussed below, that the sum-integral difference has an exponentially-suppressed volume dependence, scaling as  $e^{-mL}$ . We neglect such dependence throughout this review as it is numerically small in practice. Thus the only source of power-law volume dependence is the  $s$ -channel loop shown explicitly in Eq. (4). This can be simplified by doing the  $\ell^0$  integral, and then replacing the sum with the integral plus sum-integral difference. One then obtains

$$i\mathcal{M}_{2L} = i\mathcal{M}_2 - \frac{\lambda^2}{2} \left[ \frac{1}{L^3} \sum_{\vec{\ell}} - \int \frac{d^3\vec{\ell}}{(2\pi)^3} \right] \frac{i}{2\omega_{\vec{\ell}} 2\omega_{P-\vec{\ell}}(E - \omega_{\vec{\ell}} - \omega_{P-\vec{\ell}} + i\epsilon)} + \mathcal{O}(e^{-mL}, \lambda^3), \quad (5)$$

where  $\omega_{\vec{\ell}} \equiv \sqrt{m^2 + \vec{\ell}^2}$ .

We next set  $\vec{P} = 0$  and consider the weak coupling limit,  $|\mathcal{M}_2| \ll 1$ . Then the two-particle energy will be very close to the lowest-lying non-interacting state,  $E = 2m + \mathcal{O}(\lambda)$ . In this regime, the dominant volume-dependent contribution to  $\mathcal{M}_{2L}$  comes from the  $\vec{\ell} = 0$  contribution to the sum, leading to

$$i\mathcal{M}_{2L} = i\mathcal{M}_2 - \frac{\lambda^2}{2} \frac{1}{L^3} \frac{i[1 + \mathcal{O}(1/L)]}{4m^2(E - 2m + i\epsilon)} + \dots \quad (6)$$

At this stage we identify a problem with the truncated expression. While the leading-order term contains no poles, the next-to-leading order result contains a pole at the non-interacting level  $E = 2m$ . Both results are incorrect for the interacting theory. The problem arises because, for  $E - 2m = \mathcal{O}(\lambda)$ , the first two terms are effectively of the same order. More importantly, some of the terms we have neglected are of this order as well.

To resolve the issue we must include all diagrams with any number of  $s$ -channel bubbles, as shown in **Figure 1(b)**. Doing so leads to a geometric series, and summing this leads to a shift in the pole in  $\mathcal{M}_{2L}$ . To see this explicitly, we work to all orders in  $\lambda/(E - 2m)$  while only working to leading-order in the scattering amplitude (so that  $\mathcal{M}_2 = -\lambda$ ). We find

$$\mathcal{M}_{2L} = \mathcal{M}_2 \sum_{n=0}^{\infty} \left( \frac{(-1)}{2L^3} \frac{[1 + \mathcal{O}(1/L)]}{4m^2(E - 2m + i\epsilon)} \mathcal{M}_2 \right)^n = \frac{\mathcal{M}_2(E - 2m)}{E - 2m + \mathcal{M}_2/(8m^2L^3) + \mathcal{O}(1/L^4)}. \quad (7)$$

If we now make the replacement  $\mathcal{M}_2 = -32\pi m a$ , valid at leading order in  $\lambda$  for all  $s$  (and to all orders in  $\lambda$  for  $s = 4m^2$ ), then we find that the pole is indeed shifted to the position given in Eq. (2).

**2.1.2. Example: quantization condition in 1 + 1 dimensions.** Our second example shows how the quantization condition emerges for general values of  $E$  and  $L$ . Working in 1 + 1 dimensions keeps the essential features of the derivation while simplifying the calculation. For simplicity, we restrict to the c.m. frame,  $\vec{P} = 0$ , and drop the argument  $P$  in  $\mathcal{M}_2$  and related quantities.

It is instructive to first show how the unitarity relation arises diagrammatically. To this end, we expand  $\mathcal{M}_2$  in powers of the Bethe-Salpeter (BS) kernel, as shown in **Figures 1(c)-(d)**. This

**Threshold shift:**  
Example of a shifted pole in the finite-volume correlator

kernel is the sum of all diagrams that are two-particle irreducible in the  $s$ -channel. Thus it contains loops with three or more particles, and single-particle poles, but no two-particle loops. We focus on the kinematic region  $m < E < 3m$ , within which the BS kernel has no on-shell cuts, and thus is real. Thus the only sources of imaginary contributions are the two-particle loops, which can have on-shell cuts. Performing the time component integrals, the expression for  $\mathcal{M}_2$  can be brought into the form<sup>6</sup>

$$i\mathcal{M}_2(p', p) = \sum_{n=0}^{\infty} \prod_{j=0}^{n-1} \left( \frac{1}{2} \int_{k_{j+1}} iB_2(k_j, k_{j+1}) \frac{i}{(2\omega_{k_j})^2 (E - 2\omega_{k_j} + i\epsilon)} \right) iB_2(k_n, p) \Big|_{k^0=p'}. \quad (8)$$

Here we have left the momenta  $p'$  and  $p$  general. We now set these on-shell, via  $p' = p = q^*$ , and drop the dependence on the left-hand side.

We are interested in extracting the imaginary part. Thus we use the identity relating the  $i\epsilon$  prescription to a principal value (PV) prescription plus an imaginary  $\delta$ -function term:

$$\mathcal{M}_2 = \sum_{n=0}^{\infty} \left( -B_2 \otimes \left[ \mathcal{I}_{\text{PV}} - \frac{1}{2} \int_k \frac{i}{(2\omega_k)^2} \delta(E - 2\omega_k) \right] \otimes \right)^n B_2, \quad (9)$$

where  $\otimes$  indicates integration of adjacent quantities over the common momentum, and  $\mathcal{I}_{\text{PV}}$  is the pole term with the PV prescription. Thus factors of  $B_2$  adjacent to  $\otimes$  are evaluated off shell. By contrast, those adjacent to the delta-function can be set on shell, i.e. with  $2\omega_{k_j} = E$ .

Performing the integral we find

$$\mathcal{M}_2 = \sum_{n=0}^{\infty} \left( [-B_2 \otimes \mathcal{I}_{\text{PV}} \otimes] + B_2 \frac{i}{8pE} \right)^n B_2. \quad (10)$$

The sum on the right-hand side with the imaginary term dropped leads precisely to the K matrix,  $\mathcal{K}_2$ , where we stress that the external arguments of the  $B_2$ s are on shell. Reorganizing the full right-hand side, keeping the imaginary term, thus gives

$$\mathcal{M}_2 = \sum_{n=0}^{\infty} \left( \sum_{m=0}^{\infty} [-B_2 \otimes \mathcal{I}_{\text{PV}} \otimes]^m B_2 \frac{i}{8q^*E} \right)^n \sum_{p=0}^{\infty} [-B_2 \otimes \mathcal{I}_{\text{PV}} \otimes]^p B_2, \quad (11)$$

$$= \sum_{n=0}^{\infty} \left( -\mathcal{K}_2 \left[ -\frac{i}{8q^*E} \right] \right)^n \mathcal{K}_2 = \frac{1}{\mathcal{K}_2^{-1} - i/(8q^*E)}, \quad (12)$$

where again it is crucial that the  $B_2$ s next to the  $i/(8q^*E)$  terms are on shell, so that it is the on-shell  $\mathcal{K}_2$  that appears. The final result is simply the unitarity relation, Eq. (1), but written in one spatial dimension.

We now argue that a similar analysis can be applied to the finite-volume correlator  $\mathcal{M}_{2L}$  introduced above. We recall that  $\mathcal{M}_{2L}$  is a real function of energy whose poles give the finite-volume spectrum of the theory. The first step is to note that  $\mathcal{M}_{2L}$  is given by Eq. (8), except that the integrals are replaced by finite-volume sums over  $k_j = 2\pi n_j/L$ , with  $n_j$  an arbitrary integer, and the  $i\epsilon$  is dropped. This is shown diagrammatically in **Figure 1(e)-(f)**. The BS kernels in  $\mathcal{M}_{2L}$  are, strictly speaking, the finite-volume versions, but these differ from those in infinite volume only by exponentially-suppressed terms, a difference we neglect. This holds in our kinematic regime because the loops inside  $B_2$  have integrands that cannot go on shell, and are thus nonsingular. One can then use the Poisson summation formula to show that the sum-integral difference is exponentially suppressed. This result holds in any number of dimensions, and was first derived in Ref. (10).

We now follow analogous steps to the demonstration of unitarity shown above, except that here we separate the sum over finite-volume modes into the principal-value integral and the residual sum-integral difference (instead of separating the  $i\epsilon$ -integral into a PV integral and an imaginary part):

$$\mathcal{M}_{2L} = \sum_{n=0}^{\infty} \left( [-B_2 \otimes \mathcal{I}_{\text{PV}} \otimes] - B_2 \otimes \frac{1}{2} \left[ \frac{1}{L} \sum_k -\text{PV} \int \frac{dk}{2\pi} \right] \frac{1}{(2\omega_k)^2 (E - 2\omega_k)} \otimes \right)^n B_2, \quad (13)$$

$$= \sum_{n=0}^{\infty} \left( [-B_2 \otimes \mathcal{I}_{\text{PV}} \otimes] - B_2 \frac{1}{4EL} \frac{L^2}{4\pi^2} \left[ \sum_n -\text{PV} \int dn \right] \frac{1}{x^2 - n^2} \right)^n B_2 + \mathcal{O}(e^{-mL}), \quad (14)$$

where in the second line we have rearranged the expression and introduced  $x \equiv q^*L/(2\pi)$ .

Unlike in our derivation of the unitarity relation, here we have no Dirac delta function to project  $B_2$  to its on-shell value. Nonetheless, we note that the factors of the BS kernels in the  $L$ -dependent

<sup>6</sup>This requires a redefinition of  $B_2$  to absorb the ‘‘Z-diagram’’ contribution from two-particle loop, as well as the residue function of the remaining pole.

---

**Unitarity of  $\mathcal{M}_2$ :**  
1 + 1-dimensional  
case

---



---

**Key result:** BS  
kernels have  
exponentially-  
suppressed  $L$   
dependence

---

terms can, in fact be evaluated at  $k = q^*$ . This is justified because the difference is exponentially suppressed

$$\left[ \frac{1}{L} \sum_k -\text{PV} \int \frac{dk}{2\pi} \right] \frac{\omega_k}{(2\omega_k)^2(q^{*2} - k^2)} [B_2(p'', k)B_2(k, p') - B_2(p'', q^*)B_2(q^*, p')] =$$

$$\left[ \frac{1}{L} \sum_k - \int \frac{dk}{2\pi} \right] \frac{\omega_k}{(2\omega_k)^2(q^{*2} - k^2)} [b(k)(q^{*2} - k^2)] \propto \sum_{n' \neq 0} \int \frac{dk}{2\pi} \frac{b(k)e^{iLkn'}}{\sqrt{k^2 + m^2}} = \mathcal{O}(e^{-mL}). \quad (15)$$

**On-shell projection:**  
from sum-integral  
difference

The first line here shows the difference between on- and off-shell BS kernels and, on the second line, we have used the result that this must equal a smooth function (denoted  $b(k)$ ) times  $q^{*2} - k^2$ . Canceling the pole, and then using the Poisson summation formula, we have rewritten the result as a series of Fourier transforms with respect to integer multiples of  $L$ . This leads to our conclusion that kernels can be placed on shell up to terms that we neglect. In this way we have an effective delta function, in place of the true factor of  $\delta(E - 2\omega)$  that appeared in the unitarity derivation.

Following the remaining steps exactly as above, and using  $\mathcal{K}_2^{-1} = q^* \cot \delta(q^*) / (8q^{*2}E)$ , we find

$$\mathcal{M}_{2L} = \frac{8q^*E}{\cot \delta(q^*) + \cot \phi(q^*, L)}, \quad (16)$$

where

$$\cot \phi(q^*, L) \equiv \frac{x}{\pi} \left[ \sum_n -\text{PV} \int dn \right] \frac{1}{x^2 - n^2} = \frac{x}{\pi} \frac{\pi \cot(\pi x)}{x} = \cot \frac{q^*L}{2}, \quad (17)$$

and the second equality follows by noting that the principal-value integral is identically zero and the sum can be evaluated analytically. This implies that the finite-volume spectrum is given by all solutions to

$$\cot \delta(q^*) + \cot \frac{q^*L}{2} = 0, \quad (18)$$

equivalently

$$e^{2i\delta(q^*) + iq^*L} = 1, \quad (19)$$

**Quantization  
condition in 1 + 1  
dimensions:**

which is the well-known result for 1+1-dimensional theories (31).

These simplified cases illustrate the key steps in the derivation of the quantization conditions:

#### Key steps

1. Demonstrate that power-like finite-volume dependence arises only from  $s$ -channel diagrams.
2. Sum contributions from all Feynman diagrams to identify the shift in the finite-volume energies.

**2.1.3. General derivation of two-particle quantization condition.** This was first presented in the seminal work of Lüscher (10, 11), but the approach followed here is more closely based on the derivation of Ref. (33).

We begin with the BS equation for the two-particle scattering amplitude

$$\mathcal{M}_2 = \mathbf{B}_2 + \mathbf{B}_2 \otimes \mathcal{I} \otimes \mathcal{M}_2, \quad (20)$$

shown diagrammatically in **Figure 1(c)**. Here we have introduced a boldface notation in which coordinate dependence, and factors of  $i$ , are suppressed, e.g.  $\mathbf{B}_2 \equiv iB_2(P; k'; k)$ . The symbol  $\otimes \mathcal{I} \otimes$  here indicates an integral over the two-particle loop, now in 3 + 1 dimensions,

$$\mathbf{B}_2 \otimes \mathcal{I} \otimes \mathcal{M}_s \equiv \frac{1}{2} \int \frac{d^4k}{(2\pi)^4} iB_2(P; k''; k') \frac{iz(k')}{k'^2 - m^2 + i\epsilon} \frac{iz(P - k')}{(P - k')^2 - m^2 + i\epsilon} i\mathcal{M}_2(P; k'; k), \quad (21)$$

where  $z(k)/(k^2 - m^2 + i\epsilon)$  is the fully dressed propagator, normalized so that  $z = 1$  on shell.

To determine the finite-volume spectrum, we again use  $\mathcal{M}_{2L}$ , although, in fact, any finite-volume correlator would suffice [a different choice was made in Ref. (33)]. We now use the result described above that the finite- and infinite-volume versions of the BS kernel differ by terms scaling as  $e^{-mL}$  if  $m < E^* < 3m$  (or  $0 < E^* < 4m$  is there is a  $\mathbb{Z}_2$  symmetry separating even- and odd-particle number sectors). This result allows us to write the BS equation for the finite-volume correlator [shown in **Figure 1(e)**]:

$$\mathcal{M}_{2L} = \mathbf{B}_2 + \mathbf{B}_2 \otimes \mathcal{S} \otimes \mathcal{M}_{2L}, \quad (22)$$

$$\mathbf{B}_2 \otimes \mathcal{S} \otimes \mathcal{M}_{2L} \equiv \frac{1}{2} \int \frac{dk'^0}{2\pi} \frac{1}{L^3} \sum_{\vec{k}'} iB_2(P; k''; k') \frac{iz(k')}{k'^2 - m^2 + i\epsilon} \frac{iz(P - k')}{(P - k')^2 - m^2 + i\epsilon} i\mathcal{M}_{2L}(P; k'; k). \quad (23)$$



Here the finite-volume momentum  $\vec{k}'$  is summed over the values  $2\pi\vec{n}/L$ , with  $\vec{n}$  a vector of integers. We next replace the sum with an integral and a sum-integral difference. All power-like  $L$  dependence lies in the latter quantity. As in the 1 + 1-dimensional analysis above, and as shown in detail in Refs. (33, 17), the sum-integral difference picks out the on shell values of the quantities on either side of  $\mathcal{S}$ . Specifically, it is found that

$$\mathbf{B}_2 \otimes \mathcal{S} \otimes \mathcal{M}_{2L} = \mathbf{B}_2 \otimes \mathcal{I} \otimes \mathcal{M}_{2L} + \mathbf{B}_2 \mathbf{F}_2^{i\epsilon} \mathcal{M}_{2L} \quad (24)$$

$$\mathbf{B}_2 \mathbf{F}_2^{i\epsilon} \mathcal{M}_{2L} \equiv iB_{2;\ell''m'';\ell'm'}(P) iF_{2;\ell''m'';\ell'm'}^{i\epsilon}(P, L) i\mathcal{M}_{2L;\ell'm';\ell m}(P), \quad (25)$$

$$iF_{2;\ell''m'';\ell'm'}^{i\epsilon}(P, L) \equiv \frac{1}{2} \left[ \frac{1}{L^3} \sum_{\vec{k}} - \int \frac{d^3\vec{k}}{(2\pi)^3} \right] \frac{i\mathcal{Y}_{\ell''m''}(\vec{k}^*) \mathcal{Y}_{\ell'm'}^*(\vec{k}^*)}{2\omega_k 2\omega_{P-k} (E - \omega_\ell - \omega_{P-k} + i\epsilon)}. \quad (26)$$

where the product in the second line is now a matrix product with indices given by the angular momentum in the c.m. frame of the two on-shell particles. The quantity  $F_2^{i\epsilon}$  is a matrix of geometric functions that encodes how angular momentum-states mix due to the reduced symmetry of the finite-volume system.<sup>7</sup> It is the generalization to three-spatial dimensions of the simple one-dimensional sum evaluated in Eq. (17). We have introduced  $\mathcal{Y}_{\ell m}(\vec{k}^*) = \sqrt{4\pi}(k^*/q^*)^\ell Y_{\ell m}(\hat{k}^*)$ , where the prefactor multiplying the spherical harmonic removes spurious singularities near  $\vec{k}^* = \vec{0}$ .

At this stage the derivation proceeds by substituting Eq. (24) into Eq. (22) and rearranging

$$\mathcal{M}_{2L} = \mathbf{B}_2 + \mathbf{B}_2 [\otimes \mathcal{I} \otimes + \mathbf{F}_2^{i\epsilon}] \mathcal{M}_{2L}, \quad (27)$$

$$= \sum_{n=0}^{\infty} \mathbf{B}_2 \left[ [\otimes \mathcal{I} \otimes + \mathbf{F}_2^{i\epsilon}] \mathbf{B}_2 \right]^n, \quad (28)$$

$$= \sum_{n=0}^{\infty} \left( \sum_{n'=0}^{\infty} \mathbf{B}_2 [\otimes \mathcal{I} \otimes \mathbf{B}_2]^{n'} \right) \left[ \mathbf{F}_2^{i\epsilon} \left( \sum_{n'=0}^{\infty} \mathbf{B}_2 [\otimes \mathcal{I} \otimes \mathbf{B}_2]^{n'} \right) \right]^n, \quad (29)$$

$$= \sum_{n=0}^{\infty} \mathcal{M}_2 [\mathbf{F}_2^{i\epsilon} \mathcal{M}_2]^n = \mathcal{M}_2 \frac{1}{1 - \mathbf{F}_2^{i\epsilon} \mathcal{M}_2}. \quad (30)$$

In the first line we have substituted the identity for  $\mathcal{S}$ , Eq. (24). Then we have iteratively substituted the expression for  $\mathcal{M}_{2L}$  to display all volume dependence. In the third line we have regrouped into separate sums over  $\mathcal{I}$  and  $\mathbf{F}_2^{i\epsilon}$ . In the final step, we have identified the sums involving  $\mathcal{I}$  with  $\mathcal{M}_2$ , using Eq. (20). Alternatively, one can formally solve Eq. (27) directly for  $\mathcal{M}_{2L}^{-1}$

$$\mathcal{M}_{2L}^{-1} = [\mathbf{B}_2^{-1} - \otimes \mathcal{I} \otimes] - \mathbf{F}_2^{i\epsilon}, \quad (31)$$

and identify the square-bracketed contribution as  $\mathcal{M}_2^{-1}$ . But since the final step is difficult to justify without an all-orders expansion in  $\mathbf{B}_2$ , it is not clear to us that this more direct line adds anything to the derivation.

We deduce that, for fixed values of  $\vec{P}$  and  $L$ , the finite-volume energy spectrum in the region  $E^* < 3m$  is given (up to  $e^{-mL}$  corrections) by all solutions in  $E$  to the quantization condition

$$\det_{\ell'm';\ell m} [\mathcal{M}_2^{-1}(E^*) + F_2^{i\epsilon}(E, \vec{P}, L)] = 0, \quad (32)$$

where  $\mathcal{M}_{2;\ell'm';\ell m} = \delta_{\ell'\ell} \delta_{m'm} \mathcal{M}_2^{(\ell)}$ . The extensions to multiple coupled two-particle channels, including different species and particles with spin, are known, as reviewed in Ref. (12).

In the following it will be useful to express the quantization condition in terms of the K matrix. To this end we introduce a version of  $F_2$  in which the PV prescription is used in the integral in Eq. (26) rather than the  $i\epsilon$  prescription. We denote this simply as  $F_2$  without a superscript. It is straightforward to show [see, e.g., Ref. (17)] that the quantization condition (32) can be exactly rewritten as

$$\det_{\ell'm';\ell m} [\mathcal{K}_2^{-1}(E^*) + F_2(E, \vec{P}, L)] = 0, \quad (33)$$

where  $\mathcal{K}_{2;\ell'm';\ell m} = \delta_{\ell'\ell} \delta_{m'm} \mathcal{K}_2^{(\ell)}$ .

## 2.2. Three-particle quantization condition in the RFT approach

We now turn to the derivation of the three-particle quantization condition, presented in Refs. (17, 18).

As is discussed in detail in those publications, the quantization condition depends on an intermediate quantity, referred to as a divergence-free three-particle K matrix and denoted by  $\mathcal{K}_{\text{df},3}$ . This is a non-standard object that encodes the short-distance part of the three-particle scattering amplitude. It has the same degrees of freedom as the standard scattering amplitude but

<sup>7</sup>Both the sum and integral must be UV-regulated. The choice of regulator is unimportant, however, as different choices lead to results for  $F_2^{i\epsilon}$  differing only by exponentially suppressed terms.  $F_2^{i\epsilon}$  is related to the generalized zeta functions defined in Ref. (10, 11); the explicit relation is given, e.g., in Ref. (41).

---

$F_2^{i\epsilon}(P, L)$ : Matrix of geometric functions describing  $L$  dependence.

---



---

**Two-particle result:** Lüscher quantization condition for two-particle states.

---



---

**Two-particle quantization condition:** K-matrix form

---

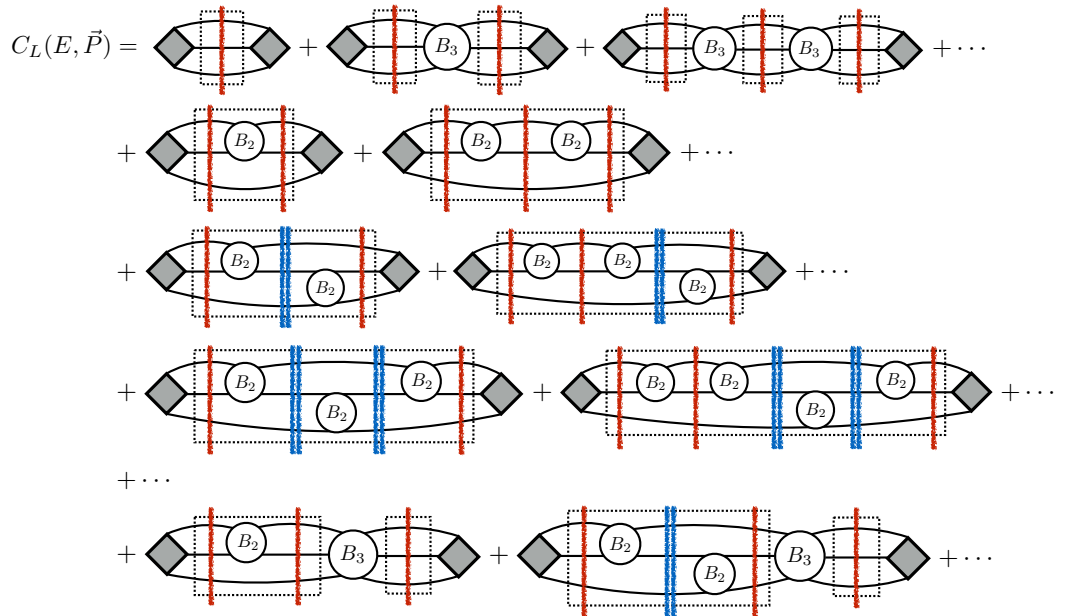


**Figure 2**

Skeleton expansion for finite-volume correlator  $C_L$ . Filled triangles indicate the vacuum-to-three-particle matrix elements of the creation and annihilation operators, called  $i\sigma^{\dagger*}$  and  $i\sigma^*$ , respectively, in the text. Solid lines are fully dressed propagators with unit on-shell residue. Unfilled circles are infinite-volume BS kernels  $B_2$  and  $B_3$ , as indicated. Dashed rectangles enclose three-momenta that are summed. In the subsequent analysis, sums are replaced by integrals plus sum-integral differences in places denoted by the red vertical lines, and this leads to so-called  $F$  cuts. Where the interacting pair switches, there is a contribution in which the sum is kept explicit, and this leads to the geometric quantity  $G$ . The places where this occurs are indicated by double blue vertical lines.

should be easier to extract from the finite-volume spectrum, since it is a smooth, real function. Most importantly, its relation to the standard  $\mathbf{3} \rightarrow \mathbf{3}$  scattering amplitude,  $\mathcal{M}_3$ , is known (18) and depends only on the on-shell  $\mathbf{2} \rightarrow \mathbf{2}$  scattering amplitude. Thus, the envisioned work-flow is summarized by

$$E_n(L) \implies \mathcal{K}_{\text{df},3} \mathcal{M}_2 \implies \mathcal{M}_3. \quad (34)$$

In this section we sketch the derivation of the quantization condition for three identical relativistic scalar particles. Following Refs. (17, 18), we restrict attention to theories with a  $\mathbb{Z}_2$  symmetry that decouples the even- and odd-particle-number sectors. In addition we assume that the two-particle  $K$  matrices have no poles in the kinematic region of interest. An example of such a theory is the  $3\pi^+$  system in QCD in the isospin limit, where  $G$ -parity plays the role of the  $\mathbb{Z}_2$  symmetry, and the  $2\pi^+$  subsystem is not resonant. The generalizations to include  $\mathbf{2} \rightarrow \mathbf{3}$  scattering and to describe systems with sub-channel resonances (generating  $K$ -matrix poles) have been worked out in Refs. (19) and (20), respectively.

The derivation we present is a simplified version of that given in Ref. (17), based on the improved approach introduced in Ref. (20). We focus on the important steps, pointing the reader to Refs. (17, 20) for detailed justifications. We begin in Sec. 2.2.1 by setting up the strategy of the derivation, based on a skeleton-expansion of a finite-volume correlation function,  $C_L$ . In Sec. 2.2.2 we summarize how the  $L$  dependence is isolated for diagrams of all topologies. We then, in Sec. 2.2.3, combine results to reach a closed form for  $C_L$ , from which immediately follows the quantization condition in terms of  $\mathcal{K}_{\text{df},3}$ . Finally, in Sec. 2.2.4 we review the relation between  $\mathcal{K}_{\text{df},3}$  and  $\mathcal{M}_3$ .

**2.2.1. Preliminaries.** As in the two-particle case, the derivation presented here is carried out to all perturbative orders in a generic, relativistic quantum field theory. By “generic” we mean that no assumptions about the vertices or power-counting scheme are required.

Consider the finite-volume correlation function

$$C_L(E, \vec{P}) \equiv \int_L d^4x e^{-iEt+i\vec{P}\cdot\vec{x}} \langle \sigma(x) \sigma^\dagger(0) \rangle_L, \quad (35)$$

where  $\sigma^\dagger(0)$  has odd-particle quantum numbers. In the region  $m < E^* < 5m$  (where  $m$  is the physical particle mass and  $E^* = \sqrt{E^2 - \vec{P}^2}$ ), all power-like  $L$ -dependence arises from intermediate three-particle states.

With this in mind, in Ref. (17) we construct a skeleton expansion in terms of BS kernels and fully dressed propagators, as shown in **Figure 2**. The expansion is entirely motivated by the goal of displaying all important  $L$ -dependence, equivalently all on-shell or long-distance intermediate

**Basic work-flow:**  
Relating the  
finite-volume  
energies to  $\mathcal{M}_3$ .

**Finite-volume  
correlator:** Poles give  
spectrum

states. The final structure can be expressed in terms of two kernels:  $B_2$ , already used above, and  $B_3$ , which contains all 3-particle irreducible diagrams in three-to-three scattering (as well as one-particle propagation that introduces no singularities in the kinematic window considered). Both  $B_2$  and  $B_3$  have only exponentially suppressed  $L$  dependence, and thus, under the approximation guiding the derivation, can be replaced by their infinite-volume counterparts.

As we explain in more detail in the following, the relevant volume-dependence, generated by sums over  $\vec{k} = 2\pi\vec{n}/L$  in the loops of the skeleton expansion, can be expressed in terms of two finite-volume geometric functions, denoted  $F$  and  $G$ . The first is closely related to the zeta-function of Eq. (26) and is defined in terms of the PV version of that quantity:<sup>8</sup>

$$F_{k'\ell'm';k\ell m}(P, L) \equiv \delta_{k'k} H(\vec{k}) F_{2,\ell'm,\ell m}(P - k, L). \quad (36)$$

Here we display the indices that all matrices in the three-particle quantization condition share:  $\vec{k}$ ,  $\ell$ , and  $m$ . These can be understood by separating the three particles into a dimer [called “scattering pair” in Ref. (17)] and a spectator.<sup>9</sup> The spectator is constrained to have one of the discrete finite-volume momenta,  $\vec{k} = 2\pi\vec{n}/L$ , while the dimer is decomposed into angular momentum states in its c.m. frame (as was done in the two-particle quantization condition), leading to the  $\ell m$  indices. The  $\delta_{k'k}$  in Eq. (36) thus represents a situation in which the spectator does not interact. The argument of  $F_2$  gives the four-momentum flowing through the dimer,  $(P - k)^\mu = (E - \omega_k, \vec{P} - \vec{k})$ .

A new feature in Eq. (36) is the appearance of the cutoff function  $H(\vec{k})$ . For fixed  $P$ , as  $|\vec{k}|$  increases, the dimer c.m. energy,

$$E_{2,k}^* = \sqrt{(E - \omega_k)^2 - (\vec{P} - \vec{k})^2}, \quad (37)$$

passes below threshold  $E_{2,k}^* = 2m$  and eventually drops to zero. For technical reasons explained in Ref. (17) the formalism requires that  $E_{2,k}^{*2} \geq 0$ . The cutoff function  $H(\vec{k})$  accomplishes this by smoothly varying from unity at and above threshold to zero when  $E_{2,k}^* = 0$ . An explicit example of the cutoff is given in Ref. (17), but will not be needed here. One can think of it as a soft cutoff at  $|\vec{k}| \sim m$ .

The presence of  $H(\vec{k})$  implies that the index  $\vec{k}$  runs over a finite number of values. The full matrix space remains infinite dimensional, however, due to the angular-momentum degrees of freedom. If these are truncated, as is common practice in the two-particle sector, then  $F$  reduces to a finite-dimensional matrix.

The locations in the diagrams of the skeleton expansion at which an  $F$  appears is shown in **Figure 2**. A quantization condition based only on  $F$  would predict three-particle energies of the form  $E_n(L) = \omega_k + E_2(L, \vec{P} - \vec{k})$  where the second term is an interacting two-particle level with the indicated momentum. Of course, for three identical particles, this cannot be the correct spectrum. It properly encodes the interactions of two, but neglects the third which enters as a non-interacting constituent, albeit with the proper relativistic energy. This motivates the appearance of the second geometric function,  $G$ , that encodes the volume effects of an exchange in the scattering pair. The explicit definition is<sup>10</sup>

$$G_{p\ell'm';k\ell m} \equiv \left(\frac{k^*}{q_p^*}\right)^{\ell'} \frac{4\pi Y_{\ell'm'}(\hat{k}^*) H(\vec{k}) H(\vec{p}) Y_{\ell m}^*(\hat{p}^*)}{(P - p - k)^2 - m^2} \left(\frac{p^*}{q_k^*}\right)^\ell \frac{1}{2\omega_k L^3}, \quad (38)$$

where  $\vec{k}^*$  is  $\vec{k}$  boosted to the dimer c.m. frame when  $\vec{p}$  is the spectator momentum, and  $q_p^* = \sqrt{E_{2,p}^{*2}/4 - m^2}$  is the momentum of each of the two dimer constituents when  $\vec{p}$  is the spectator momentum and all particles are on shell. The same definitions hold for  $\vec{p}^*$  and  $q_k^*$ , with the roles  $\vec{k}$  and  $\vec{p}$  exchanged. Examples of the locations in skeleton-expansion diagrams that lead to factors of  $G$  are shown in **Figure 2**.

At this stage we are left to explain three more-technical aspects of the notation. First, at various intermediate stages we consider sums over three-to-three diagrams in which an incoming or outgoing particle is singled-out by the property of being *unscattered* by the outermost two-to-two insertion. We use the superscript ( $u$ ) to denote such unsymmetrized quantities. Given that we consider identical particles, the final result cannot (and, as we prove in Ref. (17), does not) depend on these incomplete objects. Second, we find it convenient to introduce a bold-faced notation for the BS kernels as well as other building blocks defined via partial diagrammatic sums. This simply denotes that factors of  $i$  and  $1/(2\omega L^3)$  have been absorbed to simplify expressions, and is taken over from Ref. (20). Third, it is convenient to begin the derivation by studying only the part of  $C_L(E, \vec{P})$  that survives when we send  $B_3 \rightarrow 0$ . This is indicated by a  $[B_2]$  superscript,  $C_L \rightarrow C_L^{[B_2]}$ .

With these preliminaries established, we are now ready to jump into the derivation.

<sup>8</sup>The PV version is used since this leads to a quantization condition involving  $\mathcal{K}_2$  instead of  $\mathcal{M}_2$  [as in Eq. (33)], and thus avoids the cusps in  $\mathcal{M}_2$  that can lead to power-law finite-volume dependence (17).

<sup>9</sup>The term “dimer” can potentially lead to confusion as different definitions appear in the literature. In this work a dimer is simply a pair of particles projected to a definite orbital angular momentum.

<sup>10</sup>In Refs. (17, 18) a slightly different form of  $G$  was used, in which the pole term has the form of that in the definition of  $F_2$ , Eq. (26). The difference between the two pole terms is nonsingular, and can be absorbed by a change in the definition of  $\mathcal{K}_{\text{df},3}$ . It was later realized that using the relativistic form shown here leads to a  $\mathcal{K}_{\text{df},3}$  that is relativistically invariant (19).

---

**Kinematic function**  
 $F$ : Related to  $F_2$

---



---

**Kinematic function**  
 $G$ : Arises from exchange of scattering pair

---

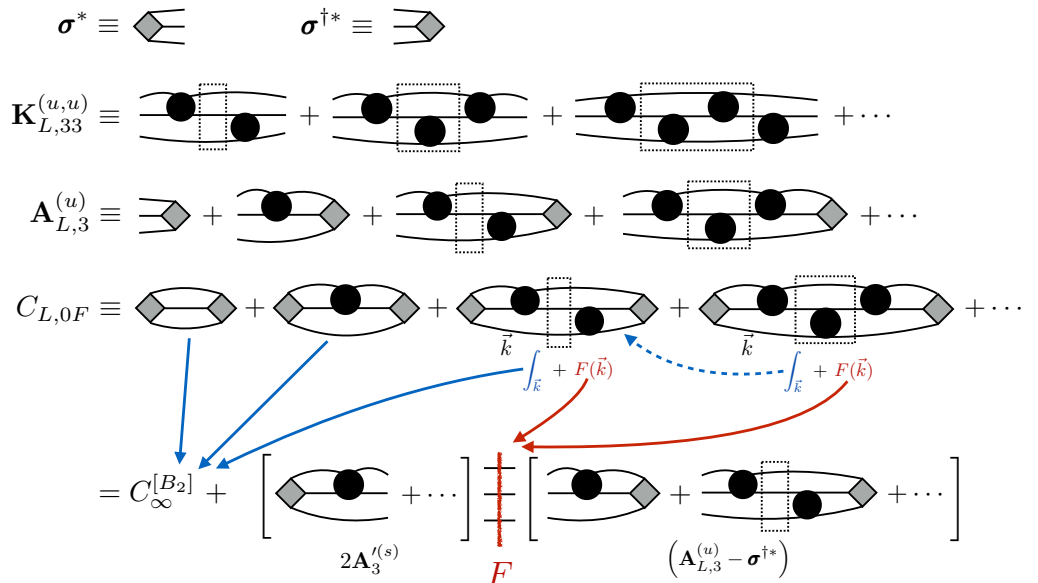


**Figure 3**

Definitions of quantities appearing in Eq. (39), using notation from previous figures. Filled circles represent two-particle K matrices,  $\mathbf{K}_2$ . The quantity  $\mathbf{A}_{L,3}^{(u)}$  is given by the horizontal reflection of the diagrams for  $\mathbf{A}_{L,3}$ . Also shown is a sketch of the derivation of the decomposition of  $C_{L,0F}$  given in Eq. (41), in which the sum over the left-most summed loop integral is replaced by an integral plus sum-integral difference, the latter leading to a factor of  $\mathbf{F}$ . For the integral term, if there are further sums remaining, then the procedure is repeated, as indicated by the dashed blue arrow.

**2.2.2. Decomposing to the level of  $\mathbf{K}_{\text{df}}$ .** We begin with Eq. (174) of Ref. (17), expressed in boldface notation as in Eq. (49) of Ref. (20),

$$C_L^{[B_2]} = C_{L,0F} - \frac{2}{3} \boldsymbol{\sigma}^* \mathbf{F} \boldsymbol{\sigma}^{\dagger*} + \mathbf{A}_{L,3}^{(u)} \mathbf{F}_{33}^{(0)} \sum_{n=0}^{\infty} \left( \mathbf{K}_{L,33}^{(u,u)} \mathbf{F}_{33}^{(0)} \right)^n \mathbf{A}_{L,3}^{(u)}, \quad (39)$$

$$\mathbf{F}_{33}^{(0)} \equiv \mathbf{F} \frac{1}{1 - \mathbf{K}_2 \mathbf{F}}. \quad (40)$$

To obtain this result we have applied the method that led to the two-particle quantization condition for diagrams in which adjacent factors of  $B_2$  are attached to the same dimer. This explains the appearance of  $\mathbf{K}_2 \equiv i[2\omega L^3] \mathcal{K}_2$ , which is diagonal in spectator indices,<sup>11</sup> as well as  $\mathbf{F} \equiv iF/(2\omega L^3)$ .

The other quantities in Eq. (39) involve diagrams in which particles pairwise scatter via  $\mathbf{K}_2$ , with the remaining loops (containing exchange propagators) involving sums over the finite-volume momenta. These quantities are finite-volume objects, as indicated by the subscript  $L$ . They are shown **Figure 3**. Specifically,  $\mathbf{K}_{L,33}^{(u,u)}$  is sum of all fully connected three-to-three scattering diagrams involving alternating pairwise scattering, while  $\mathbf{A}_{L,3}^{(u)}$ ,  $\mathbf{A}_{L,3}^{(u)}$  and  $C_{L,0F}$  are defined similarly, but with additional endcap factors  $\boldsymbol{\sigma}^{\dagger*}$  and  $\boldsymbol{\sigma}^*$ .

The remaining task is to decompose the volume dependence of  $C_{L,0F}$ ,  $\mathbf{A}_{L,3}^{(u)}$ ,  $\mathbf{A}_{L,3}^{(u)}$  and  $\mathbf{K}_{L,33}^{(u,u)}$ , expressing each object as matrix products of infinite-volume quantities and finite-volume geometric functions. To this end one can show that

$$C_{L,0F} = C_{\infty}^{[B_2]} + 2\mathbf{A}_3^{l(s)} \mathbf{F} (\mathbf{A}_{L,3}^{(u)} - \boldsymbol{\sigma}^{\dagger*}), \quad (41)$$

$$\mathbf{A}_{L,3}^{l(u)} = \mathbf{A}_3^{l(u)} + 2\mathbf{A}_3^{l(s)} \mathbf{F} \left( \mathbf{K}_{L,33}^{(u,u)} + \mathbf{K}_2 \right), \quad (42)$$

$$\mathbf{A}_{L,3}^{(u)} = \mathbf{A}_3^{(u)} + \left( \mathbf{K}_{L,33}^{(u,u)} + \mathbf{K}_2 \right) \mathbf{F} 2\mathbf{A}_3^{(s)}, \quad (43)$$

thereby reducing all unfactorized  $L$ -dependence to that of  $\mathbf{K}_{L,33}^{(u,u)}$ . The derivation of the result for  $C_{L,0F}$  is sketched in **Figure 3**; those for the other quantities is similar. The idea is to move from left to right, replacing a given momentum sum with an integral plus a sum-integral difference. The term with the difference leads to a factor of  $\mathbf{F}$  whereas that with the integral is further decomposed, by applying the same prescription to the next sum in the chain. In this way all contributions are cast into the same form: an  $\mathbf{F}$ -cut with an infinite-volume expression to the left and remaining  $L$  dependence to the right.

<sup>11</sup>For technical reasons, in the subthreshold region ( $E_{2,k}^* < 2m$ ),  $\mathcal{K}_2$  is defined to include a smooth interpolation from the sub-threshold K matrix ( $\propto [q^* \cot \delta]^{-1}$ ) to the sub-threshold scattering amplitude ( $\propto [q^* \cot \delta + |q^*|]^{-1}$ ).

**Initial decomposition:**  
Factorizing  $L$ -dependence between adjacent  $\mathbf{K}_2$  factors.

**Second decomposition:**  
Reducing all terms to  $\mathbf{K}_{L,33}^{(u,u)}$ .

At this stage it only remains to decompose  $\mathbf{K}_{L,33}^{(u,u)}$ . One finds

$$\mathbf{K}_{L,33}^{(u,u)} = \mathbf{K}_{L,33}^{(0)} + [1 + \mathbf{T}\mathbf{G}]\mathbf{K}_{\text{df},33}^{(u,u)} \frac{1}{1 - \mathbf{G}\mathbf{K}\mathbf{K}_{\text{df},33}^{(u,u)}} [1 + \mathbf{G}\mathbf{T}], \quad (44)$$

where

$$\mathbf{K}_{L,33}^{(0)} \equiv \frac{1}{1 - \mathbf{K}_2\mathbf{G}}\mathbf{K}_2\mathbf{G}\mathbf{K}_2, \quad \mathbf{T} \equiv \mathbf{K}_2 \frac{1}{1 - \mathbf{G}\mathbf{K}_2}, \quad \mathbf{G}\mathbf{K} \equiv \frac{1}{1 - \mathbf{G}\mathbf{K}_2}\mathbf{G}. \quad (45)$$

This decomposition, explained in Ref. (20), leads to the first appearance of the second geometric function  $\mathbf{G} = i(2\omega L^3)^{-1}G$ , as well of the intermediate infinite-volume quantity  $\mathbf{K}_{\text{df},33}^{(u,u)} = i\mathcal{K}_{\text{df},3}^{(u,u)}$ . Here the subscript “df” stands for divergence free and indicates that kinematic singularities present in the three-to-three scattering amplitude are absent from this quantity.

**2.2.3. Combining and symmetrizing.** We now substitute all decompositions into Eq. (39) and organize terms by the number  $\mathbf{K}_{\text{df},33}$  factors that they contain.

Beginning with the  $\mathbf{K}_{\text{df}}$ -independent contributions, note that  $\mathbf{K}_{L,33}^{(u,u)} \rightarrow \mathbf{K}_{L,33}^{(0)}$  in the limit of  $\mathbf{K}_{\text{df},33} \rightarrow 0$ . This can be used to show that the factor appearing between  $\mathbf{A}'_{L,3}$  and  $\mathbf{A}_{L,3}$  in Eq. (39) reduces as

$$\mathbf{F}_{33}^{(0)} \sum_{n=0}^{\infty} \left( \mathbf{K}_{L,33}^{(u,u)} \mathbf{F}_{33}^{(0)} \right)^n \xrightarrow{\mathbf{K}_{\text{df}} \rightarrow 0} \mathbf{F} \frac{1}{1 - \mathbf{T}\mathbf{F}} \equiv \mathbf{Z}. \quad (46)$$

It is then straightforward to reduce the two endcaps as well as  $C_{L,0F}$  to reach

$$\mathbf{A}'_{L,3} \xrightarrow{\mathbf{K}_{\text{df}} \rightarrow 0} \mathbf{A}'_3 - 2\mathbf{A}'_3{}^{(s)}(1 - \mathbf{F}\mathbf{T}), \quad (47)$$

$$\mathbf{A}_{L,3} \xrightarrow{\mathbf{K}_{\text{df}} \rightarrow 0} \mathbf{A}_3 - (1 - \mathbf{T}\mathbf{F})2\mathbf{A}_3{}^{(s)}, \quad (48)$$

$$C_{L,0F} - C_{\infty}^{[B_2]} \xrightarrow{\mathbf{K}_{\text{df}} \rightarrow 0} 2\mathbf{A}_3{}^{(s)}\mathbf{F} \left( \mathbf{A}_3 - (1 - \mathbf{T}\mathbf{F})2\mathbf{A}_3{}^{(s)} - \boldsymbol{\sigma}^{\dagger*} \right). \quad (49)$$

Here we have expressed the endcaps in terms of  $\mathbf{A}'_3 \equiv \mathbf{A}'_3{}^{(u)} + \mathbf{A}'_3{}^{(s)} + \mathbf{A}'_3{}^{(t)}$  and similarly for the unprimed object. This combines the three possible choices of momentum assignment for the external particle that is not attached to the outermost  $\mathbf{2} \rightarrow \mathbf{2}$  insertion. Although we are forced to consider unsymmetrized quantities at various stages of the derivation, it is crucial that the final result should only depend on objects that have exchange symmetry with respect to the momenta of the three identical particles. This is proven explicitly for all systems considered so far in Refs. (17, 18, 19, 20).

Substituting the four relations [Eqs. (46)-(49)] into Eq. (39) leads to a complicated expression. However, the important part is given by the term containing the two symmetrized endcap factors  $\mathbf{A}'_3$  and  $\mathbf{A}_3$ :

$$C_L^{[B_2]} - C_{\infty}^{[B_2]} \supset \mathbf{A}'_3\mathbf{Z}\mathbf{A}_3 = \mathbf{A}'_3 \left[ \mathbf{F} + \mathbf{F} \frac{1}{1 - \mathbf{K}_2(\mathbf{F} + \mathbf{G})} \mathbf{K}_2\mathbf{F} \right] \mathbf{A}_3, \quad (50)$$

where in the equality we have given an alternative, expanded expression for  $\mathbf{Z}$ . Remarkably, this simple result almost captures the full volume dependence at leading order in  $\mathbf{K}_{\text{df},33}$ . The set of remaining contributions modifies the result in two minor ways. First, many of the additional terms can be proven to have only exponentially-suppressed  $L$  dependence and are absorbed into a redefinition of  $C_{\infty}^{[B_2]}$ . Second, the one additional volume cut that survives (after significant reshuffling) is a term that corrects the numerical factor multiplying  $\mathbf{A}'_3\mathbf{F}\mathbf{A}_3$ . One finds

$$C_L^{[B_2]} - C_{\infty}^{[B_2]} = \mathbf{A}'_3\mathbf{F}_{33}\mathbf{A}_3 + \mathcal{O}(\mathbf{K}_{\text{df}}), \quad (51)$$

$$\mathbf{F}_{33} \equiv \frac{1}{3}\mathbf{F} + \mathbf{F} \frac{1}{1 - \mathbf{K}_2(\mathbf{F} + \mathbf{G})} \mathbf{K}_2\mathbf{F}. \quad (52)$$

As we will see below,  $\mathbf{F}_{33}$ , which combines geometric functions together with factors of  $\mathcal{K}_2$ , is the three-particle analog of  $\mathbf{F}_2$ . It is the central object entering the three-particle quantization condition.

We now continue the pattern by considering the next order in  $\mathbf{K}_{\text{df},33}$ . For example, from the decomposition of  $\mathbf{K}_{L,33}^{(u,u)}$  in Eq. (44) together with the  $\mathbf{K}_{\text{df}}$ -independent result [Eq. (46)] it is straightforward to show that

$$\mathbf{F}_{33}^{(0)} \sum_{n=0}^{\infty} \left( \mathbf{K}_{L,33}^{(u,u)} \mathbf{F}_{33}^{(0)} \right)^n = \mathbf{Z} + \mathbf{Z}(1 + \mathbf{T}\mathbf{G})\mathbf{K}_{\text{df},33}^{(u,u)}(1 + \mathbf{G}\mathbf{T})\mathbf{Z} + \mathcal{O}(\mathbf{K}_{\text{df}}^2). \quad (53)$$

The next step is to identify the  $\mathcal{O}(\mathbf{K}_{\text{df}})$  contributions to  $\mathbf{A}'_{L,3}$ ,  $\mathbf{A}_{L,3}$  and  $C_{L,0F} - C_{\infty}^{[B_2]}$  and assemble all terms to identify the corresponding contribution to  $C_L^{[B_2]} - C_{\infty}^{[B_2]}$ . However, for the purposes of this review, we think it more instructive to consider a single contribution to  $C_L^{[B_2]}$ , given by sandwiching the  $\mathcal{O}(\mathbf{K}_{\text{df}})$  part of Eq. (53) between symmetrized, infinite-volume endcaps,

$$\mathbf{A}'_3\mathbf{Z}(1 + \mathbf{T}\mathbf{G})\mathbf{K}_{\text{df},33}^{(u,u)}(1 + \mathbf{G}\mathbf{T})\mathbf{Z}\mathbf{A}_3 = \mathbf{A}'_3 \left[ \mathbf{F} + \mathbf{F} \frac{1}{1 - \mathbf{K}_2(\mathbf{F} + \mathbf{G})} \mathbf{K}_2(\mathbf{F} + \mathbf{G}) \right] \mathbf{K}_{\text{df},33}^{(u,u)} \left[ \mathbf{F} + (\mathbf{F} + \mathbf{G})\mathbf{K}_2 \frac{1}{1 - (\mathbf{F} + \mathbf{G})\mathbf{K}_2} \mathbf{F} \right] \mathbf{A}_3. \quad (54)$$

---

**Final decomposition:**  
Displaying all  $L$  dependence as products of geometric functions.

---



---

**Leading order result:**  
 $C_L^{[B_2]}$  at leading order in  $\mathbf{K}_{\text{df}}$ .

---

---

**NLO result:**  $C_L^{[B_2]}$  at next-to-leading order in  $\mathbf{K}_{\text{df}}$ .

---

As above, the inclusion of all other terms leads to only minor modifications to this key result. Again various  $L$ -independent terms are absorbed, not only into  $C_\infty^{[B_2]}$  but also into  $\mathbf{A}'_3$  and  $\mathbf{A}_3$ . A new feature that arises here is that the unsymmetrized  $\mathbf{K}$  matrix,  $\mathbf{K}_{\text{df},33}^{(u,u)}$ , can be replaced with a symmetrized form, up to a correction of the symmetry factor on the isolated  $\mathbf{F}$  term ( $\mathbf{F} \rightarrow \mathbf{F}/3$ ) and a modification of the cuts multiplying  $\mathbf{K}_{\text{df},33}^{(u,u)}$ . The upshot is that the square-bracketed factors are replaced with  $\mathbf{F}_{33}$ , the same three-particle volume cut that appeared at the previous order:

$$C_L^{[B_2]} - C_\infty^{[B_2]} = \mathbf{A}'_3 \mathbf{F}_{33} \mathbf{A}_3 + \mathbf{A}'_3 \mathbf{F}_{33} \mathbf{K}_{\text{df},33}^{[B_2]} \mathbf{F}_{33} \mathbf{A}_3 + \mathcal{O}(\mathbf{K}_{\text{df}}^2). \quad (55)$$

At this stage, we see the structure emerging and can assign a physical interpretation to the pattern. Within the finite-volume correlator, the three-particle state is created with an insertion of  $\mathbf{A}_3$ . This is equal to a matrix element of  $\sigma^\dagger$  and measures the probability amplitude to create a three-particle state from the vacuum.<sup>12</sup> The three particles then propagate and rescatter in the box, leading to a pattern of Feynman diagrams that translates into a set of nested geometric series.

We organize these in powers of the short-distance three-to-three interaction,  $\mathbf{K}_{\text{df},33}$ . Then at leading order the volume effects arise due to a single insertion of  $\mathbf{F}_{33}$ . This, in turn, is equal to a factor of  $\mathbf{F}$  together with a sum over all terms of the form  $\mathbf{F} \mathbf{K}_2 \mathbf{F} \mathbf{K}_2 \mathbf{G} \cdots \mathbf{F} \mathbf{K}_2 \mathbf{F}$  where either  $\mathbf{F}$  or  $\mathbf{G}$  can appear between any two factors of  $\mathbf{K}_2$ . The sum over all such terms represents the fact that any particle pair can scatter (inducing a factor of  $\mathbf{K}_2$ ) and then propagate between consecutive re-scattering events (giving  $\mathbf{F}$ ), or alternatively exchange the scattering pair (leading to  $\mathbf{G}$ ). Finally the term that is linear in  $\mathbf{K}_{\text{df},33}$  is governed by this same structure, together with the observation that a short-distance three-particle interaction may arise anywhere in the series of two-particle scattering events.

From the physical intuition it is perhaps not so surprising that the same pattern continues to all orders in  $\mathbf{K}_{\text{df}}$ . This is proven explicitly in Refs. (17) and (20). In addition, the inclusion of the three-particle BS kernels turns out to only modify the definition of the divergence-free  $\mathbf{K}$  matrix. This can be accommodated by replacing  $\mathbf{K}_{\text{df},33}^{[B_2]}$  with  $\mathbf{K}_{\text{df},33}$ . Putting all this together leads to the main result of Ref. (17)

$$C_L - C_\infty = \sum_{n=0}^{\infty} \mathbf{A}'_3 \mathbf{F}_{33} \left[ \mathbf{K}_{\text{df},33} \mathbf{F}_{33} \right]^n \mathbf{A}_3 = \mathbf{A}'_3 \mathbf{F}_{33} \frac{1}{1 - \mathbf{K}_{\text{df},33} \mathbf{F}_{33}} \mathbf{A}_3. \quad (56)$$

Thus the poles in the finite-volume correlator occur whenever the matrix appearing between  $\mathbf{A}'_3$  and  $\mathbf{A}_3$  has a divergent eigenvalue. We deduce that, for fixed values of  $\vec{P}$  and  $L$ , the finite-volume energy spectrum in the region  $m < E^* < 5m$  is given (up to  $e^{-mL}$  corrections) by all solutions in  $E$  to the quantization condition

$$\det_{\vec{k}' \ell' m'; \vec{k} \ell m} \left[ \mathcal{K}_{\text{df},3}(E^*) + F_3(E, \vec{P}, L)^{-1} \right] = 0. \quad (57)$$

---

**Three-particle quantization condition:** RFT approach

---

Here we have returned to the non-bold notation, using  $\mathbf{F}_{33} = iF_3$  and  $\mathbf{K}_{\text{df},33} = i\mathcal{K}_{\text{df},3}$ , that we will use for the remainder of the discussion.

**2.2.4. Relating  $\mathcal{K}_{\text{df},3}$  to  $\mathcal{M}_3$ .** In the previous sections we have related  $\mathcal{K}_{\text{df},3}(E^*)$  to the finite-volume energy spectrum. This object can, in principle, be constrained by calculating finite-volume energies, for example from the Euclidean-time decay of correlators calculated numerically using LQCD, and then applying Eq. (57). Of course, this is only of interest if  $\mathcal{K}_{\text{df},3}(E^*)$  can be related to infinite-volume observables.

Indeed, as was shown in Ref. (18), this modified  $\mathbf{K}$  matrix is related to the three-to-three scattering amplitude via an integral equation that depends only on known functions as well as the on-shell two-particle scattering amplitude. The relation has a number of desirable features. The equations are defined at fixed energy, meaning that  $\mathcal{K}_{\text{df},3}(E^*)$  is only required for  $E^*$  where the physical scattering amplitude is to be determined. In addition once the quantization condition is fixed, there is no ambiguity or scheme dependence in the relation between  $\mathcal{K}_{\text{df},3}$  and  $\mathcal{M}_3$ . Finally the  $\mathcal{K}_{\text{df},3}$  to  $\mathcal{M}_3$  relation manifestly encodes the complicated unitarity constraints of the three-particle scattering amplitude (34).

The relation is derived in a slightly round-about way. In particular we show in Ref. (18) that one can define an alternative finite-volume correlation function,  $\mathcal{M}_{3L}$ , that becomes the physical scattering amplitude in a carefully constructed  $L \rightarrow \infty$  limit. This new correlator differs from  $C_L$  only in the interpolating fields. As a result it admits a similar skeleton expansion and a similar decomposition into geometric functions. In Ref. (18) we show that

$$\mathcal{M}_{3L}[\mathcal{K}_{\text{df},3}, \mathcal{K}_2] \equiv \mathcal{S} \left[ \mathcal{D}_L^{(u,u)} - \mathcal{L}_L^{(u)} \frac{1}{1 + \mathcal{K}_{\text{df},3} F_3} \mathcal{K}_{\text{df},3} \mathcal{R}_L^{(u)} \right], \quad (58)$$

---

<sup>12</sup>Strictly speaking this does not hold because of the removal of singular long-distance contributions. To recover the standard matrix element these have to be put back in, following an approach analogous to the relation between  $\mathcal{K}_{\text{df},3}$  and  $\mathcal{M}_3$  discussed in Sec. 2.2.4 below.

where  $\mathcal{D}_L^{(u,u)}$ ,  $\mathcal{L}_L^{(u)}$  and  $\mathcal{R}_L^{(u)}$  are known explicitly, and are closely related to  $F_3$ , while  $\mathcal{S}$  indicates symmetrization.

As an aside, we observe from Eq. (58) that we can use  $\mathcal{M}_{3L}$  instead of  $C_L$  in order to derive the quantization condition, as its poles lie at the same positions. Indeed, the unsymmetrized quantity in square braces is very similar to the dimer-particle scattering amplitude used in the alternative approaches to deriving the quantization condition discussed below.

We now obtain  $\mathcal{M}_3$  by taking a judiciously chosen  $L \rightarrow \infty$  limit of  $\mathcal{M}_{3L}$ . This requires that factors of  $i\epsilon$  in the pole terms be first put back in, so the  $L \rightarrow \infty$  limit is well defined. Thus we have

$$\mathcal{M}_3(\mathcal{K}_{\text{df},3}, \mathcal{K}_2) = \lim_{\epsilon \rightarrow 0} \lim_{L \rightarrow \infty} \mathcal{M}_{3,L}(\mathcal{K}_{\text{df},3}, \mathcal{K}_2), \quad (59)$$

which gives a set of purely infinite-volume integral equations, given explicitly in Ref. (18). These map the real, short-distance three-body quantity  $\mathcal{K}_{\text{df},3}$  to the complex, unitary, relativistic three-to-three scattering amplitude.

### 2.3. Truncating the quantization condition

The quantization condition Eq. (57) is a formal result, because the determinant runs over an infinite-dimensional matrix space. This is exactly as in the two-particle case and, in direct analogy to that case, truncating  $\mathcal{K}_2$  and  $\mathcal{K}_{\text{df},3}$  to vanish above some  $\ell_{\text{max}}$  is sufficient to reduce all matrices in the quantization condition to have finite dimension (17). Specifically, the matrices then have dimension  $[(2\ell_{\text{max}} + 1) \times N_{\vec{k}}]$  where  $N_{\vec{k}}$  is the number of finite-volume momenta,  $\vec{k}$ , for which the cutoff function,  $H(\vec{k})$ , is non-zero.

The simplest approximation is to take  $\ell_{\text{max}} = 0$ : the  $s$ -wave approximation. This is the approximation used from the beginning in the alternative approaches described below. It assumes that  $\mathcal{K}_2$  and the dimer within  $\mathcal{K}_{\text{df},3}$  are both dominated by  $s$ -wave interactions. Given this truncation,  $\mathcal{K}_2$  reduces to a single function of the two-particle CM energy, whereas  $\mathcal{K}_{\text{df},3}$  retains dependence on the spectator momenta  $\vec{k}^{*}$  and  $\vec{k}^*$ . This is the form of the RFT quantization condition that is used in the comparison with the results from alternate approaches; it is given explicitly in Eq. (88) below.

The  $s$ -wave approximation is well motivated at energies close to the three-particle threshold, since higher waves are then suppressed by factors of  $(q_k^*)^\ell$ . To study this systematically, one expands  $\mathcal{K}_2$  and  $\mathcal{K}_{\text{df},3}$  about threshold in powers of  $s - 9m^2$  and related quantities. For  $\mathcal{K}_2$  this leads to the effective range expansion, with the leading term being the scattering length. The expansion of  $\mathcal{K}_{\text{df},3}$  is constrained because it is relativistically invariant, symmetric under initial and final particle interchange, and time reversal invariant (19). Using these symmetries, one can show that the first two terms in the expansion are not only pure  $s$ -wave but also isotropic, i.e. independent of the spectator momenta (19, 35, 36). At third order one must include  $d$ -wave contributions in both  $\mathcal{K}_2$  and  $\mathcal{K}_{\text{df},3}$  (36).

The  $s$ -wave approximation plus isotropic  $\mathcal{K}_{\text{df},3}$  is referred to as the isotropic approximation. In this most extreme truncation  $\mathcal{K}_{\text{df},3}$  depends only on  $E^*$ , so we can write

$$\mathcal{K}_{\text{df},3} = \delta_{\ell,0} \delta_{m,0} |1\rangle \mathcal{K}_{\text{df},3}^{\text{iso}}(E^*) \langle 1|, \quad (60)$$

where  $|1\rangle$  is an unnormalized vector with unit entry for every active spectator momentum. If one further restricts to the  $A_1$  irreducible representation (irrep) of the cubic group, then, as shown in Ref. (17), all nontrivial solutions to the quantization condition satisfy

$$\mathcal{K}_{\text{df},3}^{\text{iso}}(E^*) = -1/F_3^{\text{iso}}(E, \vec{P}, L), \quad F_3^{\text{iso}} \equiv \langle 1|F_{3,s}|1\rangle, \quad (61)$$

where  $F_{3,s}$  is the form of  $F_3$  after  $s$ -wave truncation [see Eq. (88)]. Thus, in this approximation, we recover a one-to-one correspondence between finite-volume energy levels and the value of  $\mathcal{K}_{\text{df},3}^{\text{iso}}(E^*)$ . This approximation has been studied numerically in Ref. (37), and some of the results are shown in Sec. 4 below.

### 2.4. Analytic investigations of the RFT quantization condition

In this subsection we describe two analytic investigations of the three-particle quantization condition, Eq. (57). The main aim is to check the formalism by comparing to known results in special limits, but a side-benefit is that some new analytic results are obtained.

**2.4.1.  $1/L$  expansion.** Without interactions, the lowest energy state of three particles with  $\vec{P} = 0$  has energy  $3m$ . Turning on interactions, this level will shift to  $E_0(L)$ . For sufficiently large  $L$ ,  $E_0(L) - 3m$  can be expanded in powers of  $1/L$ , the so-called threshold expansion. The leading term scales as  $1/L^3$ , corresponding to the probability of two particles to overlap, while three-particle interactions enter first at  $1/L^6$ . This expansion was worked out previously, using NRQM, up to  $\mathcal{O}(1/L^7)$  (38, 39, 40).

We determined the threshold expansion, starting from Eq. (57), in Ref. (41). We found<sup>13</sup>

$$E_0(L) = 3m + \frac{12\pi a}{mL^3} \left\{ 1 - \mathcal{I} \frac{a}{\pi L} + \left( \frac{a}{\pi L} \right)^2 (\mathcal{I}^2 + \mathcal{J}) + \frac{64\pi^2 a^2}{mL^3} \mathcal{C}_3 + \frac{3\pi a}{m^2 L^3} + \frac{6\pi r a^2}{L^3} \right. \\ \left. + \left( \frac{a}{\pi L} \right)^3 \left( -\mathcal{I}^3 + \mathcal{I}\mathcal{J} + 15\mathcal{K} + \frac{16\pi^3}{3} (3\sqrt{3} - 4\pi) \log\left(\frac{mL}{2\pi}\right) + \mathcal{C}' \right) \right\} - \frac{\mathcal{M}_{3,\text{thr}}}{48m^3 L^6} + \mathcal{O}\left(\frac{1}{L^7}\right), \quad (62)$$

where we have introduced the following geometric constants:  $\mathcal{I} = -8.914$ ,  $\mathcal{J} = 16.532$ ,  $\mathcal{K} = 8.402$ ,  $\mathcal{C}_3 = -0.05806$ ,  $\mathcal{C}' = 2052$ , whose origin is explained in Ref. (41). The scattering parameters that enter here are the scattering length,  $a$ , the effective range,  $r$ , and the threshold three-to-three scattering amplitude  $\mathcal{M}_{3,\text{thr}}$ . The latter has a somewhat subtle definition, due to the fact that the full scattering amplitude diverges at threshold and thus requires a subtraction. Again see Ref. (41) for details. Note that the leading term is three times that found in Eq. (2) for the two-particle system, as expected since there are three pairs of particles that can interact.

The result of Eq. (62) agrees with the results of Refs. (38, 39) for the terms through  $\mathcal{O}(1/L^5)$ . This provides a strong check on the formalism. Relativistic effects enter at  $\mathcal{O}(1/L^6)$  and here no general check is available. However the  $\log L$  term is universal and its coefficient also agrees with earlier work. To check the remaining  $1/L^6$  terms, in Refs. (42, 43) we calculated  $E_0(L)$  in  $\lambda\phi^4$  theory up to  $\mathcal{O}(\lambda^4)$ , finding complete agreement with Eq. (62). Working at this order checks all the terms entering at  $1/L^6$ .

We also note that, for weakly interacting systems, the threshold expansion might provide a partial alternative to the full quantization condition. By fitting the  $L$  dependence of the threshold state at many volumes, one could in principle extract  $\mathcal{M}_{3,\text{thr}}$  and thereby determine the near-threshold scattering amplitude. This approach has been followed successfully in  $\lambda\phi^4$  theory in the recent work of Ref. (44).

**2.4.2. Volume-dependence of a three-body bound state.** Our second analytic result concerns the volume-dependence of a non-relativistic three-scalar Efimov bound state (45) in the unitarity limit for two-particle interactions, i.e. with  $1/a \rightarrow 0$ . This was studied in Ref. (46) using non-relativistic quantum mechanics in a finite-volume. The authors found that, when the infinite volume system contains a bound state, then the lowest lying state in finite volume has energy

$$E_B(L) = 3m - \frac{\kappa^2}{m} + \Delta E(L), \quad (63)$$

where  $\kappa$  is the binding momentum, and

$$\Delta E(L) = c|A|^2 \frac{\kappa^2}{m} \frac{1}{(\kappa L)^{3/2}} e^{-2\kappa L/\sqrt{3}} + \dots \quad (64)$$

Here the ellipsis indicates terms suppressed by additional factors of  $\kappa^2/m^2$  or  $1/(\kappa L)$  as well as faster-decaying exponentials. The result depends on  $c \simeq -96.351$ , a known geometric constant, and  $|A|^2$ . The latter is a normalization correction that arises because the asymptotic wave-function is not a strict solution to the Schrödinger equation. It is expected to be close to unity when the pairwise interactions of the theory are well-described by a short-range potential.

The generic relativistic quantization condition presented above, Eq. (57), holds for systems with a three-particle bound state, as long as there are no bound dimers. Indeed, in our numerical implementation in the isotropic approximation, we have found that the formalism can support such bound states (37). Assuming the existence of such a state (i.e. that there is a subthreshold pole in  $\mathcal{M}_3$ ), in Ref. (47) we were able to provide another check on the quantization condition by reproducing the coefficient, power-law envelope and exponential decay given by Eq. (64). In addition we extended the result to non-zero momentum in the finite-volume frame, and found that the moving-frame energy is shifted according to

$$\Delta E(\vec{P}, L) = f_3[\vec{n}] \Delta E(L) + \dots, \quad f_3[\vec{n}] = \frac{1}{6} \sum_{\hat{s}} e^{i(2\pi/3)\hat{s}\cdot\vec{n}}, \quad (65)$$

where  $\vec{n} = L\vec{P}/(2\pi)$  and the sum runs over the six unit vectors pointing along the finite-volume axes. An interesting corollary is that the leading-order volume shift vanishes for  $\vec{n} = (0, 1, 1)$ .

### 3. ALTERNATIVE APPROACHES

As noted in the Introduction, two other approaches for deriving the three-particle quantization condition have been used, and in this section we describe them, quote the resulting form for the quantization condition, and explain in what ways these approaches agree with and differ from the

<sup>13</sup>In Ref. (41) we write  $\mathcal{C}_F + \mathcal{C}_4 + \mathcal{C}_5$  in place of  $\mathcal{C}'$ .



generic RFT approach described in the previous section. In particular, we present new results concerning the analytic relation between the three approaches in the  $s$ -wave approximation, which is the only case that has been worked out explicitly within the new approaches.

We discuss the two other approaches in historical order, beginning with that based on non-relativistic effective field theory (NREFT), introduced in Refs. (21, 22), and then describing the approach based on extending the form of amplitudes required to satisfy unitarity to finite volume (23). We refer to the latter as the “finite-volume unitarity” (FVU) approach.

### 3.1. NREFT approach

NREFT is applicable when the momenta of all particles are in the non-relativistic domain,  $|\vec{p}| \ll m$ . In this regime there is no particle creation, which greatly simplifies the diagrammatic analysis. Examples where it is directly applicable in a three-particle context include three pions close to threshold in an isospin-symmetric world (so that  $G$ -parity forbids three-to-two transitions) and three nucleons close to threshold.

The first calculations using NREFT to determine finite-volume properties of three-particle systems were numerical calculations for the triton (48, 49) and Efimov states (50). This approach was then used in Refs. (21, 22) to develop the three-particle quantization condition, which we review in the following.

The authors consider a theory of identical scalars (i.e. the same setup as used in the RFT analysis presented earlier) for which the NREFT Lagrangian is<sup>14</sup>

$$\mathcal{L} = \psi^\dagger \left( i\partial_0 + \frac{\nabla^2}{2m} \right) \psi + \mathcal{L}_2 + \mathcal{L}_3, \quad (66)$$

$$\mathcal{L}_2 = -\frac{1}{2}C_0\psi^\dagger\psi^\dagger\psi\psi + \frac{1}{4}C_2\left(\psi^\dagger\overleftrightarrow{\nabla}^2\psi^\dagger\psi\psi + \text{h.c.}\right) + \dots, \quad (67)$$

$$\mathcal{L}_3 = -\frac{1}{6}D_0\psi^\dagger\psi^\dagger\psi^\dagger\psi\psi\psi + \frac{1}{12}D_2\left(\psi^\dagger\psi^\dagger\overleftrightarrow{\nabla}^2\psi^\dagger\psi\psi\psi + \text{h.c.}\right) + \dots, \quad (68)$$

where h.c. indicates hermitian conjugate,  $\overleftrightarrow{\nabla} = (\overrightarrow{\nabla} - \overleftarrow{\nabla})/2$  is the Galilean-invariant derivative, and derivatives act only on adjacent objects. The field  $\psi$  only destroys particles, since there is no corresponding antiparticle in the theory. NREFT is an expansion in  $|\vec{p}|^2/m^2$ , and thus interaction terms are classified by the number of derivatives, with the constraint from Bose symmetry that only an even number is allowed. Thus the ellipses in Eqs. (67) and (68) indicate terms with four or more derivatives, at which order arise the first terms that lead to  $d$ -wave interactions between pairs of particles. The effects of virtual particle-antiparticle pairs in the underlying relativistic theory are subsumed into the *a priori* unknown (dimensionful) constants  $C_i$  and  $D_i$ . We refer to these generically as LECs—low-energy constants.

This theory has been extensively studied in infinite volume, e.g. in its application to the three nucleon system (where the fields become fermionic and have a spin index). For a review, see Ref. (53). The LECs are to be determined by solving the two- and three-particle scattering and bound-state problems (involving the solution of integral equations) and comparing to experimental results for phase shifts and bound-state energies. One must choose a regularization, a topic with an extensive literature given the subtleties that arise in the presence of large scattering lengths (54, 55). For numerical applications, however, the standard choice is a hard cutoff,  $|\vec{p}| < \Lambda$ , and this is what is used in Refs. (21, 22).

The overall strategy employed in this approach is as follows. The NREFT is to be solved in finite volume, working first with only the leading order couplings  $C_0$  and  $D_0$ , and including higher-order terms as needed. These LECs are to be determined by comparing the theoretically predicted spectrum to that obtained in a lattice calculation. In a second step, the NREFT is then solved in infinite-volume, predicting the three-particle scattering amplitudes and bound-state properties. This approach makes use of a crucial property of the LECs, namely that they are expected to be volume-independent, since they arise from integrating out short-distance physics. Thus the values obtained in finite volume can be applied unchanged in the infinite-volume calculations.

This two-step strategy is similar to that used in the RFT analysis presented earlier, where the intermediate, cutoff-dependent quantity  $\mathcal{K}_{\text{df},3}$  was needed, and infinite-volume quantities were obtained by solving integral equations. In the NREFT approach the intermediate quantities are the LECs, which are also cutoff dependent, and thus not directly physical. What the NREFT approach provides in addition is a systematic power-counting scheme, valid as long as one works in the NR regime.

An important technical point discussed in Ref. (22) concerns a class of higher-order terms in  $\mathcal{L}_2$  and  $\mathcal{L}_3$  that lead to vanishing on-shell contributions to physical scattering amplitudes at tree level. An example from  $\mathcal{L}_2$  is a term leading to a vertex proportional to  $(\vec{k}^2 - \vec{p}^2)^2$ , where  $\vec{k}$  and  $\vec{p}$  are the relative momenta between the two particles in initial and final states, respectively. It is argued that one can choose the regularization such that these terms do not contribute to physical quantities

<sup>14</sup>There are also single-particle operators involving higher-order derivatives, which must be included perturbatively, along the lines of Ref. (51). Implementation of these terms is underway (52).

---

**NREFT Lagrangian:**  
Expansion in powers of  $|\vec{p}|^2/m^2$  including LECs

---



---

**Advantage of NREFT:** Systematic power-counting scheme

---

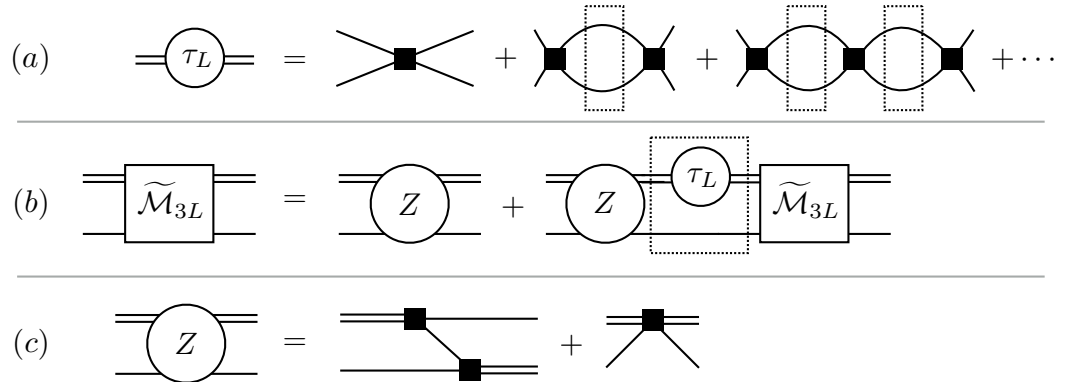


**Figure 4**

Diagrammatic representation of components of NREFT derivation of the quantization condition. As above, a dashed rectangle indicates that the three-momentum in the loop is summed over finite-volume values. Single lines are NREFT particle propagators, which are always forward in time. Double lines indicate the dimer propagator. (a) The finite-volume dimer propagator  $\tau_L$ , with filled squares representing the contributions from the interactions in  $\mathcal{L}_2$  [see Eq. (67)]. (b) Integral equation for the dimer-particulate scattering amplitude. (c) The three-particle interaction kernel  $Z$ , with filled squares representing contributions arising ultimately from interactions in  $\mathcal{L}_3$ .

**Technical result:**  
Only physical LECs need to be included

**Technical implementation:** Use of auxiliary dimer fields

even when included in loop diagrams, and thus that they can be dropped from the beginning. In this way the intermediate quantities in the NREFT approach provide a complete description of the physical amplitudes. This is the analog here of the result in the RFT formalism that the intermediate quantity  $\mathcal{K}_{\text{df},3}$  is an on-shell amplitude.

The restriction to “physical” LECs is implemented in Ref. (22) using auxiliary dimer fields. These are simply a technical device in which a composite field is introduced for two of the particles for each choice of their relative angular momentum (which here is constrained to be even). Integrating out the infinite tower of dimer fields leads back to the original Lagrangian, Eq. (66), but with only the physical LECs. The angular momentum of the dimer corresponds exactly to the indices  $\ell$  and  $m$  in the RFT approach. Details of the implementation of the dimer fields can be found in Ref. (22).

The NREFT quantization condition has been worked out explicitly so far only for the case of an  $s$ -wave dimer. This is the analog of truncating the RFT formalism to  $\ell = 0$ , an approximation described in Sec. 2.3 above. This approximation requires that the two-particle scattering amplitude vanish for all higher waves, and that the three-particle interaction does not couple to higher waves in a pair. A further restriction introduced to simplify the derivation is that  $\vec{P} = 0$ .

**3.1.1. Two-particle quantization condition.** The first step in the derivation of the three-particle quantization condition is to determine the dimer propagator in finite volume, denoted  $\tau_L(\vec{k})$  (with dependence on the total energy  $E$  kept implicit). Here  $\vec{k}$  is the spectator momentum,  $\vec{k}$ , which determines the dimer momentum to be  $\vec{P} - \vec{k} = -\vec{k}$ .  $\tau_L$  is proportional to the finite-volume scattering amplitude,  $\mathcal{M}_{2L}$ , discussed in Sec. 2.1. If we denote the  $s$ -wave component of the latter quantity, evaluated in the NR regime,<sup>15</sup> by  $\mathcal{M}_{2L,s}^{\text{NR}}(P - k)$ , where the argument denotes the dimer four-momentum, then the precise relation is

$$32\pi m \tau_L(\vec{k}) = \mathcal{M}_{2L,s}^{\text{NR}}(P - k). \quad (69)$$

The dimer propagator is given by the diagrams shown in **Figure 7(a)**. Summing the geometric series leads to

$$\tau_L(\vec{k})^{-1} = f_\tau(q_k^{*2}) + \frac{4\pi}{L^3} \sum_{\vec{a}} \frac{1}{m E_{\text{NR}} - k^2 - \vec{a}^2 - \vec{k} \cdot \vec{a}}. \quad (70)$$

Here  $f_\tau$  arises from the vertices in  $\mathcal{L}_2$ , and thus is a known function of the  $C_i$ . It is proportional to the inverse of the BS kernel. It depends on the squared relative c.m. momentum of the particles in the dimer,

$$q_k^{*2} = \frac{1}{4} \left[ (E - \omega_k)^2 - k^2 - 4m^2 \right]. \quad (71)$$

Finally,  $E_{\text{NR}} = E - 3m$  is the nonrelativistic energy, while  $\vec{a}$  is summed over the allowed finite-volume values.

We see here how the NR limit simplifies the analysis compared to that outlined in Sec. 2.1. Here there are only  $s$ -channel loops, and these contain only two particles. All the other loops in RFT collapse to the point-like interactions parametrized by the LECs. In particular, the BS kernel required in Sec. 2.1 is replaced here by the function  $1/[32\pi m f_\tau]$ . The nontrivial effort required to

<sup>15</sup>We use the phrase “in the NR regime” here and below to indicate that we keep only terms linear in  $E_{\text{NR}} = E - 3m$  and  $\vec{k}^2/(2m)$ .

show that this kernel has only exponentially suppressed volume dependence in the RFT approach is replaced here by the assumed general result from EFT that LECs are independent of volume.<sup>16</sup> With this result in hand, one simply determines the volume dependence implicitly by calculating the dimer propagator with the loop integrals replaced by sums.

The function  $f_\tau$  can be determined by considering the dimer propagator in infinite volume,  $\tau(\vec{k})$ , obtained from Eq. (70) by changing the sum into an integral with an  $i\epsilon$  prescription for the pole. Regulating the ultraviolet divergence in some manner, the integral evaluates to

$$I_\epsilon(q_k^{*2}) \equiv 4\pi \int_{\vec{a}} \frac{1}{mE_{\text{NR}} - \vec{k}^2 - \vec{a}^2 - \vec{k} \cdot \vec{a} + i\epsilon} = 4\pi \int_{\vec{a}^*} \frac{1}{\vec{q}_k^{*2} - a^{*2} + i\epsilon} = \sqrt{-q_k^{*2}} + I_{\text{PV}}(q_k^{*2}). \quad (72)$$

Here  $\int_{\vec{a}} \equiv \int d^3a/(2\pi)^3$ , and  $\vec{a}^*$  is the result of boosting  $\vec{a}$  to the dimer c.m. frame.  $I_{\text{PV}}$  is the same integral except defined using the principal-value (PV) pole prescription. Thus  $I_{\text{PV}}$  is a real, analytic function of  $q_k^{*2}$ , which in fact evaluates to a constant. The square-root in Eq. (72) is defined to have a negative imaginary part above threshold. Using these results we obtain

$$\tau(\vec{k})^{-1} = f_\tau(q_k^{*2}) + I_{\text{PV}} + \sqrt{-q_k^{*2}}, \quad (73)$$

which, when compared to the known form of the scattering amplitude [see Eq. (1) above]<sup>17</sup>

$$\tau(\vec{k})^{-1} = 32\pi m \left[ \mathcal{M}_{2,s}^{\text{NR}}(P-k) \right]^{-1} = 32\pi m \left[ \mathcal{K}_{2,s}^{\text{NR}}(q_k^*) \right]^{-1} + \sqrt{-q_k^{*2}}, \quad (75)$$

leads to the conclusion that

$$f_\tau(q_k^{*2}) + I_{\text{PV}} = 32\pi m \left[ \mathcal{K}_{2,s}^{\text{NR}}(q_k^*) \right]^{-1}. \quad (76)$$

This shows explicitly how the LECs  $C_i$ , contained in  $f_\tau$ , are related to the physical quantity  $\mathcal{K}_{2,s}$ , albeit in a cutoff dependent manner.<sup>18</sup>

Combining Eqs. (70) and (76) we obtain the final result for  $\tau_L$ ,

$$\left[ 32\pi m \tau_L(\vec{k}) \right]^{-1} = \mathcal{K}_{2,s}^{\text{NR}}(q_k^*)^{-1} + \frac{1}{8m} \left[ \frac{1}{L^3} \sum_{\vec{a}} -\text{PV} \int_{\vec{a}} \right] \frac{1}{mE_{\text{NR}} - \vec{k}^2 - \vec{a}^2 - \vec{k} \cdot \vec{a}}, \quad (77)$$

$$= \mathcal{K}_{2,s}^{\text{NR}}(q_k^*)^{-1} + F_{2,s}^{\text{NR}}(P-k, L). \quad (78)$$

The first equality is our preferred way of writing Eq. (3.2) of Ref. (22), as it shows that the volume-dependence of  $\tau_L$  arises from a sum-integral difference, just as in the analysis in Sec. 2.1.<sup>19</sup> To obtain the second equality, we note that the sum-integral difference is simply the  $s$ -wave component of  $F_2(P-k, L)$ , Eq. (26), evaluated in the NR regime, and with the  $i\epsilon$  pole prescription replaced by the PV prescription. Thus we call it  $F_{2,s}^{\text{NR}}$ , which we emphasize is a real quantity.

The two-particle quantization condition can now be obtained as an intermediate result. Energy levels are given by the positions of poles in  $\mathcal{M}_{2L}$ , leading to the algebraic result

$$\tau_L^{-1} = 0 \quad \Rightarrow \quad (\mathcal{K}_{2,s}^{\text{NR}})^{-1} + F_{2,s}^{\text{NR}} = 0. \quad (79)$$

This is equivalent to the result derived in Sec. 2.1, Eq. (33), when one keeps only the  $s$ -wave component and works in the NR regime.

**3.1.2. Three-particle quantization condition.** This is derived in Ref. (22) by considering a quantity,  $\widetilde{\mathcal{M}}_{3L}$ , the particle-dimer scattering amplitude. This is closely related to the  $s$ -wave restriction of the finite-volume three-particle amplitude,  $\mathcal{M}_{3L}$ , introduced in Sec. 2.2.4.<sup>20</sup> To obtain  $\mathcal{M}_{3L}$  from  $\widetilde{\mathcal{M}}_{3L}$ , one adds vertices at each end connecting the dimer to two particles, and then symmetrizes. This implies that, as for  $\mathcal{M}_{3L}$ , the poles of  $\widetilde{\mathcal{M}}_{3L}$  occur at the energies of three-particle finite-volume states, so that it is a good quantity to consider to derive the quantization condition. In NREFT,  $\widetilde{\mathcal{M}}_{3L}$  satisfies

$$\widetilde{\mathcal{M}}_{3L;p k} = Z_{pk} + \frac{8\pi}{L^3} \sum_{\vec{q}} Z_{pq} \tau_L(\vec{q}) \widetilde{\mathcal{M}}_{3L;q k}, \quad (80)$$

which is shown schematically in **Figure 7(b)**. Here, the subscripts  $p$ ,  $q$  and  $k$  are shorthands for

<sup>16</sup>This discussion shows that the LECs are, in general, not strictly independent of volume but instead can have an exponentially-suppressed dependence.

<sup>17</sup>The relation between the NR and relativistic versions of  $\mathcal{K}_{2,s}$  is purely kinematical, and given by

$$\mathcal{K}_{2,s}(P-k) = \sqrt{1 + q_k^{*2}/m^2} \mathcal{K}_{2,s}^{\text{NR}}(q_k^*). \quad (74)$$

<sup>18</sup>In Ref. (22), the integral is regulated by dimensional regularization, in which case  $I_{\text{PV}}$  vanishes. However, since the sums are regulated in a different manner (using a hard cutoff) we find it more consistent to use the same cutoff throughout, and thus keep  $I_{\text{PV}}$  nonvanishing. This allows us to verify explicitly that the final results of Ref. (22) are regulator independent.

<sup>19</sup>The result quoted in Ref. (22) contains only the sum, but is equivalent to that here since the corresponding integral vanishes in the regularization used in that work.

<sup>20</sup>Strictly speaking,  $\widetilde{\mathcal{M}}_{3L}$  is most closely related to the unsymmetrized amplitude  $\mathcal{M}_{3L}^{(u,u)}$  defined in Refs. (17, 18).

the corresponding spectator momenta, while the kernel  $Z_{pq}$ , shown in **Figure 7(c)**, is

$$Z_{pq} = Z_{pq}^0 + \frac{H_0(\Lambda)}{\Lambda^2} + \dots, \quad Z_{pq}^0 = \frac{1}{\vec{p}^2 + \vec{q}^2 + \vec{p} \cdot \vec{q} - mE_{\text{NR}}}. \quad (81)$$

Here  $H_0$  is a dimensionless constant proportional to  $D_0/C_0^2$ ,  $\Lambda$  is the hard cutoff on the sums, and the ellipsis represents contributions from higher order terms in  $\mathcal{L}_3$ , proportional to  $D_2$ , etc.

To use Eq. (80) one assumes that  $\mathcal{K}_{2,s}$  has been determined using the two-particle quantization condition, and thus that  $\tau_L$  is known. Since the sum over  $\vec{q}$  is cut off, Eq. (80) is a finite matrix equation for  $\widetilde{\mathcal{M}}_{3L}$ , which can be solved numerically for a given choice of the LECs. One then adjusts the LECs until the finite-volume spectrum determined from a calculation in the underlying theory (i.e. lattice QCD if considering the  $3\pi^+$  system) matches that given by Eq. (80). In practice, one should project onto irreps (irreducible representations) of the symmetry group of the cubic lattice, as described in Ref. (56), which allows a more explicit formula for the quantization condition to be given. We will, instead, provide an alternative explicit formula in the following, one that shows more clearly the relationship to the RFT result derived in the previous section.

Once one has determined the LECs as just described, a second step is required to predict the infinite-volume scattering amplitude  $\mathcal{M}_3$  and, from this, the properties of any bound states and three-particle resonances. In the NREFT approach this step is simple: one uses Eq. (80) but with  $\tau_L$  replaced by  $\tau$  and the sum replaced by an integral with an  $i\epsilon$  pole-prescription. This leads to the standard NREFT integral equation for three-particle scattering, reviewed, for example, in Ref. (53). This step is the analog of the integral equation relating  $\mathcal{K}_{\text{df},3}$  to  $\mathcal{M}_3$  described in Sec. 2.2.4.

We now comment briefly on the derivation of Eq. (80). This is conceptually just as straightforward as for two particles. This is because, in NREFT, all loops in a three-particle amplitude contain three particles, in contrast to a generic QFT in which (with a  $Z_2$  symmetry) one can have five, seven, etc. This allows one to calculate all the diagrams explicitly, without introducing auxiliary objects such as the BS kernels. In finite volume one simply replaces the integrals in these loops with momentum sums (after the time-component integral is done). LECs are again volume-independent, and summing all diagrams leads to Eq. (80).

**3.1.3. Relation to RFT approach.** It has been shown in Ref. (22) that the NREFT quantization condition described implicitly above, and the RFT quantization condition of Eq. (57), are algebraically equivalent when only the  $s$ -wave dimer is included in the latter and if only the leading order, momentum-independent, two- and three-particle interaction terms are kept, i.e. if the only nonvanishing LECs are  $C_0$  and  $D_0$ . Here we give an alternative derivation of this result that is more direct and explicit.

We begin by noting that  $Z^0$  is simply related to the switch factor  $G$  given in Eq. (38). Denoting the  $s$ -wave ( $\ell' = \ell = 0$ ) part of  $G$  in the NR regime by  $G_s^{\text{NR}}$ , one can easily show that

$$Z_{pq}^0 = -4mL^3 G_{s,pk}^{\text{NR}}. \quad (82)$$

Here we have used the fact that the cutoff functions  $H(\vec{k})$  are unity to all orders in the NR expansion. To simplify subsequent manipulations we introduce the definitions

$$\overline{\mathcal{M}}_{3L} \equiv \frac{\widetilde{\mathcal{M}}_{3L}}{4mL^3} \quad \text{and} \quad \overline{H} \equiv \frac{1}{4mL^3} \left( \frac{H_0(\Lambda)}{\Lambda^2} + \dots \right) = \overline{H}_0 + \dots \quad (83)$$

In terms of these quantities Eq. (80) can be rewritten as

$$\overline{\mathcal{M}}_{3L} = (-G_s^{\text{NR}} + \overline{H}) + (-G_s^{\text{NR}} + \overline{H})\mathcal{M}_{2L,s}^{\text{NR}}\overline{\mathcal{M}}_{3L}, \quad (84)$$

where we have also used Eq. (69). This is a matrix equation, in which all spectator-momentum indices are implicit. Solving, we find

$$\overline{\mathcal{M}}_{3L} = \frac{1}{1 - (-G_s^{\text{NR}} + \overline{H})\mathcal{M}_{2L,s}^{\text{NR}}} (-G_s^{\text{NR}} + \overline{H}), \quad (85)$$

which has a pole whenever

$$\det \left[ 1 - (-G_s^{\text{NR}} + \overline{H})\mathcal{M}_{2L,s}^{\text{NR}} \right] = 0. \quad (86)$$

This can be rewritten using Eqs. (69) and (78) as

$$\det \left[ (\mathcal{K}_{2,s}^{\text{NR}})^{-1} + F_s^{\text{NR}} + G_s^{\text{NR}} - \overline{H} \right] = 0. \quad (87)$$

Here, as in Sec. 2.2, we have elevated  $\mathcal{K}_{2,s}^{\text{NR}}$  into a diagonal matrix with entries  $\mathcal{K}_{2,s}^{\text{NR}}(q_k^*)$ , while, following Eq. (36), we denote the matrix form of  $F_{2,s}^{\text{NR}}$  by  $F_s^{\text{NR}}$ . Equation (87) is the NREFT quantization condition of Refs. (21, 22) expressed in notation similar to that of Ref. (17). Note that the expansion of  $\mathcal{K}_{2,s}$  and  $\overline{H}$  in powers of momentum has not been truncated at this stage, i.e. all the  $C_i$  and  $D_i$  are still included. The determinant is finite-dimensional because of the hard cutoff applied to the implicit spectator-momentum indices.

---

**Three-particle  
quantization  
condition in NREFT:**

---

We now compare this to the quantization condition of Ref. (17), given in Eq. (57). In the  $s$ -wave approximation, this has the form

$$\det [F_{3,s}^{-1} + \mathcal{K}_{\text{df},3,s}] = 0, \quad F_{3,s} = \frac{F_s}{2\omega L^3} \left[ \frac{1}{3} - \frac{1}{\mathcal{K}_{2,s}^{-1} + F_s + G_s} F_{2,s} \right]. \quad (88)$$

Here the subscript  $s$  indicates keeping only  $\ell' = \ell = 0$  contributions, so all quantities are matrices with only spectator-momentum indices. Note that, at this stage, the NR limit has not been taken, so the sums are cut off by the functions  $H(\vec{k})$  in  $F_s$  [see Eq. (36)] and  $G_s$  [see Eq. (38)]. By straightforward algebraic manipulations, Eq. (88) can be written in a form that looks similar to the NREFT result, Eq. (87):

$$\det [\mathcal{K}_{2,s}^{-1} + F_s + G_s - \overline{H}^R] = 0, \quad \overline{H}^R = -(\mathcal{K}_{2,s}^{-1} + G_s - 2F_s) \mathcal{K}_{\text{df},3,s} \frac{F_s}{6\omega L^3}. \quad (89)$$

Thus for the two quantization conditions to agree three conditions must be satisfied: (i) we must consider Eq. (89) in the NR regime (so that  $G_s \rightarrow G_s^{\text{NR}}$ , etc.), (ii) we must use a hard cutoff in this equation, and (iii) we must demonstrate  $\overline{H} = \overline{H}^R$ .

We consider these requirements for equivalence in turn. The spectator momenta in Eq. (89) run up to a smooth (rather than hard) cutoff at  $\Lambda^R \sim m$ . In principle, one could reduce  $\Lambda^R$  into the NR regime so that  $G_s \rightarrow G_s^{\text{NR}}$  etc. Then, setting aside the issue of  $\overline{H}$  vs.  $\overline{H}^R$ , the only difference between the results would be that between a hard and a smooth cutoff.

In practice, however, reducing  $\Lambda^R$  into the NR regime is problematic. Present calculations using LQCD are done with  $m_\pi L \sim 4 - 6$  and  $m_\pi \approx m_\pi^{\text{phys}}$ . With these parameters, even the first excited state lies outside the NR regime:

$$E_1/m_\pi = \sqrt{1 + [2\pi/(m_\pi L)]^2} \sim 1.5 - 1.9. \quad (90)$$

Thus a practical quantization condition should have its cutoff at a relativistic energy and include relativistic kinematics. In this regard, we note that Ref. (22) argue that the NREFT quantization condition can be “relativized” by including the correct kinematical factors. Indeed, we see that this can be accomplished in the present instance by replacing each of the NR quantities by their relativistic counterparts, as introduced in the RFT approach.

The final requirement for the agreement between the two quantization conditions,  $\overline{H} = \overline{H}^R$ , is, at first sight, more problematic.  $L^3 \overline{H}$  is an infinite-volume quantity, while  $L^3 \overline{H}^R$  is not, since it contains  $G_s$  and  $F_s$ . In addition,  $\overline{H}_{pq}$  is, by construction, a smooth function of  $\vec{p}$  and  $\vec{q}$ , while the presence of  $G_s$  and  $F_s$  implies that there are singularities in  $\overline{H}^R$ .<sup>21</sup> It turns out that these issues can be resolved if one (a) takes the NR limit of Eq. (89), (b) assumes that  $\mathcal{K}_{2,s}^{\text{NR}}$  is independent of momentum, which is equivalent to keeping only the leading  $C_0$  term in the NR expansion of  $\mathcal{L}_2$ , i.e. keeping only the scattering length in the effective range approximation, and (c) assumes that  $\mathcal{K}_{\text{df},3,s}$  and  $\overline{H}$  are independent of spectator momenta. For  $\mathcal{K}_{\text{df},3,s}$ , this is the isotropic limit that holds near threshold, as discussed in Sec. 2.3. For  $\overline{H}$  this means keeping only the leading  $D_0$  term in the NR expansion of  $\mathcal{L}_3$ . In other words, we consistently keep only the leading-order terms in the NR limit.

In this combined limit,  $\mathcal{K}_{\text{df},3,s} = |1\rangle \mathcal{K}_{\text{df},3}^{\text{iso}} \langle 1|$ , with  $|1\rangle$  the unnormalized isotropic vector having a unit entry in all positions. This allows us to use the following identity

$$F_s^{\text{NR}} |1\rangle = 2F_s^{\text{NR}} |1\rangle + I_s^{\text{NR}} |1\rangle, \quad \text{with } I_{s,pk}^{\text{NR}} = \delta_{pk} \frac{I_{\text{PV}}}{16\pi m}, \quad (91)$$

together with its transpose. Recall that  $I_{\text{PV}}$  is a momentum-independent, regularization-dependent constant. Denoting the leading contribution to  $\overline{H}^R$  in the NR limit by  $\overline{H}^{\text{NR}}$ , we then find

$$\overline{H}^{\text{NR}} = -([\mathcal{K}_{2,s}^{\text{NR}}]^{-1} + I_s^{\text{NR}}) \mathcal{K}_{\text{df},3,s} \frac{[\mathcal{K}_{2,s}^{\text{NR}}]^{-1} + F_s^{\text{NR}} + G_s^{\text{NR}} - I_s^{\text{NR}} - [\mathcal{K}_{2,s}^{\text{NR}}]^{-1}}{18mL^3}. \quad (92)$$

Inserting this result into the NR form of Eq (89), the matrix inside the determinant can be written

$$\left[ 1 + \frac{([\mathcal{K}_{2,s}^{\text{NR}}]^{-1} + I_s^{\text{NR}}) \mathcal{K}_{\text{df},3,s}}{18mL^3} \right] \left[ ([\mathcal{K}_{2,s}^{\text{NR}}]^{-1} + F_s^{\text{NR}} + G_s^{\text{NR}}) - \frac{1}{18mL^3} \left[ ([\mathcal{K}_{2,s}^{\text{NR}}]^{-1} + I_s^{\text{NR}}) \mathcal{K}_{\text{df},3,s} \right] \left[ ([\mathcal{K}_{2,s}^{\text{NR}}]^{-1} + I_s^{\text{NR}}) \right] \right]. \quad (93)$$

This allows the leading NR term in the relativistic quantization condition to be written in exactly the form of the NR quantization condition, Eq. (87), with

$$\overline{H} = \overline{H}_0 = \left[ 1 + \frac{([\mathcal{K}_{2,s}^{\text{NR}}]^{-1} + I_s^{\text{NR}}) \mathcal{K}_{\text{df},3,s}}{18mL^3} \right]^{-1} \left[ ([\mathcal{K}_{2,s}^{\text{NR}}]^{-1} + I_s^{\text{NR}}) \frac{\mathcal{K}_{\text{df},3,s}}{18mL^3} \right] \left[ ([\mathcal{K}_{2,s}^{\text{NR}}]^{-1} + I_s^{\text{NR}}) \right]. \quad (94)$$

Using the fact that  $\mathcal{K}_{2,s}^{\text{NR}}$  and  $I_s^{\text{NR}}$  are proportional to the identity, it is simple to show that this

<sup>21</sup>Of course, these quantities are evaluated only for discrete, finite-volume momenta, so one will in general not hit the singularities, but the point here is that the two quantities appear to have very different momentum dependence.

---

**Relativistic quantization condition:** restricted to  $s$ -wave

---



---

**Need for relativistic kinematics in practice:**

---



---

**Key identity between  $F$  and  $G$ :** Valid in isotropic approximation

---



---

**Relation of RFT and NREFT quantization conditions:**  $s$ -wave dimers only, and in the NR limit

---

result is isotropic, as required for complete equivalence. The overall factor of  $1/(mL^3)$  also matches that in  $\overline{H}_0$  [see Eq. (83)]. Furthermore, since for any constant  $x$ , we have

$$\frac{1}{1+x|1\rangle\langle 1|}|1\rangle = |1\rangle \frac{1}{1+xN}, \quad N = \langle 1|1\rangle \propto (LA)^3, \quad (95)$$

we see that the  $L^3$  in the first factor in Eq. (94) cancels, so that the right-hand side is a volume-independent constant, as required to match  $\overline{H}_0$ .<sup>22</sup> The presence of the cutoff dependent quantity  $I^{\text{NR}}$  on the right-hand side is not an issue, because both  $H_0$  and  $\mathcal{K}_{\text{df},3,s}$  are cutoff dependent. Indeed, this result allows one to map the cutoff dependence of  $H_0$  known from NREFT to that of  $\mathcal{K}_{\text{df},3,s}$ .

**3.1.4. Summary.** The derivation of the three-particle quantization condition is dramatically simplified by using NREFT, compared to the RFT derivation described earlier. This is partly due to the fact that, so far, only the  $s$ -wave dimer has been included in the former. But the primary reasons for the simplicity are (a) that the number of diagrams is sufficiently small that one can straightforwardly include them all in a simple and explicit integral equation; and (b) that the two-step approach using intermediate quantities is embraced from the beginning. No attempt is made to explicitly find all sources of power-law volume dependence by focusing on sum-integral differences. Instead, one simply uses the same NREFT in separate finite- and infinite-volume calculations. Given point (a) above, this can be done without further approximation. An additional advantage of the NREFT approach is that it is valid also in the presence of subchannel resonances, since any volume-dependence they introduce is included automatically.

The simplicity of the NREFT approach is not available in a generic RFT, since one cannot solve the three-particle scattering problem in a generic theory. Thus one is forced to keep track of finite-volume effects explicitly, leading to a more complicated derivation, and with additional considerations required for subchannel resonances.

Of course, if both approaches are carried out correctly, they should agree when we take the NR limit of the relativistic approach. This is indeed the case, as first discussed in Ref. (22), and as shown explicitly earlier in this section.

The main drawback with the NREFT approach is simply that most three-body systems of interest in nuclear and particle physics are relativistic. We have already commented on the kinematics of three pions [see Eq. (90)]: for the volumes used in lattice QCD calculations the sum over spectator momenta necessarily lies in the relativistic domain. This conclusion appears unavoidable for applications of the three-particle quantization condition to lattice QCD.

A further comment on the NREFT approach is that, once interaction terms quartic in derivatives are included, i.e. once  $C_4$  and  $D_4$  are nonzero, then one must also include  $d$ -wave ( $\ell = 2$ ) dimers, as they enter at the same power in the NR expansion. As one goes further into the relativistic domain, many higher-order terms will be needed, and thus many higher-order dimers must be included.

In summary, for the NREFT approach to have broad utility, it is necessary both that the formalism be explicitly extended to include higher waves (which we expect to be relatively straightforward) and that the kinematics somehow be relativized. This second step is claimed also to be straightforward in Ref. (22). We think, however, that it will be important at each stage to check that the results agree with those from the RFT approach.

## 3.2. Finite-volume unitarity (FVU) approach

The third approach that has been used to derive a three-particle quantization condition aims to maintain relativistic invariance but to avoid much of the work of the diagrammatic RFT approach by using the constraints arising from unitarity (23). The starting point is a representation of  $\mathcal{M}_3$  in terms of dimers<sup>23</sup> that is explicitly unitary in the  $s$ -channel (57). Then, by a judicious replacement of integrals with sums, a representation of a quantity similar to  $\mathcal{M}_{3L}$  is obtained, and from this follows the quantization condition. As in the NREFT approach, the formalism has been worked out so far only for  $s$ -wave dimers, and for  $\vec{P} = 0$ .

**3.2.1. Two-particle quantization condition.** The discussion begins by considering the two-particle subsystems. The infinite-volume  $s$ -wave scattering amplitude is written as (57)

$$\mathcal{M}_{2,s} \equiv -v(q_1, q_2) \frac{1}{D(s_{12})} v(p_1, p_2), \quad (96)$$

where  $p_i$  and  $q_i$  are the initial and final momenta, respectively, of the scattering pair, and  $s_{12} = (p_1 + p_2)^2$ . The  $s$ -channel cut lies in  $D$ , which is thus complex, while  $v$  is a smooth, real function. By relativistic invariance, it can depend only on  $s_{12}$ , but it is convenient to write it as a function

<sup>22</sup>More precisely, this is true up to corrections suppressed by powers of  $1/(\Lambda L)$ .

<sup>23</sup>In Refs. (57, 23) the dimers are referred to as ‘‘isobars’’, but they play essentially the same technical role in the analysis, so we prefer to use the name dimer throughout.

of  $Q^2 = -(p_1 - p_2)^2 = s_{12} - 4m^2$  (using the mostly-minus metric). The form used in Ref. (24) is

$$v(p_1, p_2) = \lambda(s_{12})f(Q^2), \quad f(Q^2) = \frac{1}{1 + \exp[Q^2/4 - (1 - \Lambda/2)^2]}, \quad (97)$$

where  $\lambda$  is a smooth function and  $\Lambda$  a parameter. Unitarity determines the imaginary part of the denominator  $D$ , and the full quantity can be reconstructed using an appropriately subtracted dispersion relation. The result can be written<sup>24</sup>

$$D(s_{12}) = s_{12} - M_0^2 - \frac{\lambda(s_{12})^2}{2} \int_{\vec{q}} \frac{1}{2\omega_q} \frac{f(4\vec{q}^2)^2}{s_{12} - 4\omega_q^2 + i\epsilon}, \quad (98)$$

with  $M_0$  an additional parameter. Thus we see that the introduction of the form factor in Eq. (96) leads to its appearance as a convergence factor in the loop integral in  $D$ . The claim is that this form for  $D$ , when inserted into Eq. (96), gives the most general unitary result for  $\mathcal{M}_{2,s}$ . In applications, the form for  $\lambda(s_{12})$  must be tuned so as to match the known phase shift.

The next step is to claim that the finite-volume amplitude  $\mathcal{M}_{2L}$  is obtained simply by replacing the integral in Eq. (98) with the finite-volume momentum sum. Although the integral is frame-invariant, the sum depends on the choice of frame. Anticipating the three-particle application, we label the frame by the spectator momentum,  $\vec{k}$  (so that the dimer momentum is  $-\vec{k}$ ):

$$\mathcal{M}_{2L,s}(\vec{k}) = -v_{\text{on}}(\vec{k}) \frac{1}{D_L(\vec{k})} v_{\text{on}}(\vec{k}), \quad (99)$$

Here  $v_{\text{on}}$  is the same vertex function as appearing in Eq. (99), but the new subscript is used to emphasize that external particles are on shell. The expression for  $D_L(\vec{k})$  for general  $\vec{k}$  is given in Ref. (23), but here we show only the form for the dimer at rest:

$$D_L(\vec{k} = 0) = E_{2,k}^{*2} - M_0^2 - \frac{\lambda(E_{2,k}^{*2})^2}{2} \frac{1}{L^3} \sum_{\vec{q}} \frac{1}{2\omega_q} \frac{f(4\vec{q}^2)^2}{E_{2,k}^{*2} - 4\omega_q^2 + i\epsilon}, \quad (100)$$

where  $E_{2,k}^{*2} = (E - \omega_k)^2 - \vec{k}^2$  is the value of  $s_{12}$ . The two-particle quantization condition for a general frame is then obtained from the poles of  $\mathcal{M}_{2L}$ . Since the vertex function is nonsingular, the poles occur when

$$D_L(\vec{k}) = 0. \quad (101)$$

This is the  $s$ -wave two-particle quantization condition, which can be used to constrain the parameters in  $\lambda(s)$  and  $f(Q^2)$  given the finite-volume spectrum.

This approach can be justified by the following argument, which we describe in some detail as we have not found it given explicitly in the literature. As discussed in Sec. 2.1, power-law finite-volume behavior results only from sum-integral differences over singular summands/integrands. Unitary cuts pick out exactly those loops for which integrands have poles, because it is only by integrating across a pole (with an  $i\epsilon$  prescription) that one can obtain an imaginary part. In the present case, this can occur only for two-particle loops (as long as  $s_{12} < 16m^2$ ). Thus the unitary cuts pick out exactly those loops whose sum-integral difference leads to power-law volume effects. By writing  $\mathcal{M}_2$  in the form given by Eqs. (96) and (98) one is able to isolate the contributions from such loops. The infinite-volume quantities in these expressions,  $M_0$ ,  $v$ ,  $\lambda(s)$  and  $f(Q^2)$ , certainly involve loop contributions, but these do not have singular integrands, and so sum-integral differences are exponentially suppressed. Thus they can be used unchanged in the expression for  $\mathcal{M}_{2L}$ , Eq. (100).

We find this argument very plausible, but to be completely convinced of the conclusion we rely on the fact that the quantization condition in Eq. (101) can be shown to be equivalent to that derived above in the RFT approach. This is straightforward to show, as noted in Ref. (24), but it is useful to provide the explicit argument as the result will be used later. The key point is that  $D_L$  and  $D$  differ only by a sum-integral difference, and this can be rewritten in terms of the Lüscher zeta-function  $F_{2,s}^{i\epsilon}$ . We find that, for any choice of  $\vec{k}$ ,

$$D_L(\vec{k}) = D(\vec{k}) - v_{\text{on}}(\vec{k}) F_{2,s}^{i\epsilon}(\vec{k}) v_{\text{on}}(\vec{k}). \quad (102)$$

Note that the sum-integral difference projects the function  $f$  to its on-shell value, leading to  $F_{2,s}^{i\epsilon}$  being sandwiched between on-shell vertex functions. Using Eq. (96), we can rewrite  $D_L$  as

$$D_L(\vec{k}) = -v_{\text{on}}(\vec{k}) \left[ \mathcal{M}_{2,s}(\vec{k})^{-1} + F_{2,s}^{i\epsilon}(\vec{k}) \right] v_{\text{on}}(\vec{k}). \quad (103)$$

Finally, since  $v_{\text{on}}$  is nonsingular, the quantization condition (101) is equivalent to

$$0 = \mathcal{M}_{2,s}(\vec{k})^{-1} + F_{2,s}^{i\epsilon}(\vec{k}) = \mathcal{K}_{2,s}(\vec{k})^{-1} + F_{2,s}(\vec{k}), \quad (104)$$

where we recall that  $F_{2,s}$  differs from  $F_{2,s}^{i\epsilon}$  by using the PV pole prescription. These results are identical to the  $s$ -wave projections of the conditions given in Eqs. (32) and (33). We stress that there are no caveats to this equivalence—it is an identity that holds for all  $\vec{k}$ .

<sup>24</sup>This is equivalent to the form given in Eq. (3) of Ref. (24) after correcting a typographical error.

---

**FVU approach:**  
2-particle  
quantization  
conditions

---



---

**Equivalence of FVU  
and RFT 2-particle  
quantization  
conditions:**

---

**3.2.2. Three-particle quantization condition.** In Ref. (57) a representation of the three-particle scattering amplitude,  $\mathcal{M}_3$ , is given in the presence of a single dimer. A key component is the particle-dimer scattering amplitude, denoted  $T(\vec{p}, \vec{k})$ , with  $\vec{p}$  and  $\vec{k}$  spectator momenta. This is the relativistic version of the quantity  $\widetilde{\mathcal{M}}_3$  appearing in the NREFT derivation. It is shown in Ref. (57) that, if one assumes that  $T$  satisfies a Bethe-Salpeter-type equation

$$T(\vec{p}, \vec{k}) = B(\vec{p}, \vec{k}) - \int_{\vec{q}} B(\vec{p}, \vec{q}) \frac{1}{2\omega_q D(\vec{q})} T(\vec{q}, \vec{k}), \quad (105)$$

with  $D$  the dimer propagator introduced above, then  $\mathcal{M}_3$  is unitary as long as  $B$  takes the form

$$B(\vec{p}, \vec{q}) = B_0(\vec{p}, \vec{q}) + C(\vec{p}, \vec{q}), \quad B_0(\vec{p}, \vec{q}) \equiv -\frac{\lambda(E_{2,p}^{*2})f([P-q-2p]^2)f([P-2q-p]^2)\lambda(E_{2,q}^{*2})}{(P-p-q)^2 - m^2 + i\epsilon}, \quad (106)$$

with  $C$  a smooth function.<sup>25</sup> Comparing to the NREFT derivation, we observe that Eq. (105) is the relativistic analog of (the infinite-volume version of) Eq. (80), while  $B_0$  is the relativistic version of the kernel  $Z^0$  defined in Eq. (81). We stress that the one-particle exchange (OPE) form of  $B_0$  follows from enforcing unitarity, and not from calculating Feynman diagrams. There are no constraints on  $C$ , other than smoothness.

An important question is whether this construction of  $T$  is completely general. In other words, while it has been shown that it results in a unitary  $\mathcal{M}_3$ , is the freedom left in the function  $C$  sufficient to describe an arbitrary theory? This question is not addressed in Ref. (57). We shall assume in the following that the construction is general.

The next step in the derivation is to assert that, in order to obtain the finite-volume version of  $T$ , and thus of  $\mathcal{M}_3$ , it is sufficient (up to exponentially-suppressed contributions) to replace  $D$  with  $D_L$  and the integral in Eq. (105) with a finite-volume sum. Assuming so, then

$$T_{L;pk} = B_{pk} - \frac{1}{L^3} \sum_{\vec{q}} B_{pq} \frac{1}{2\omega_q D_L(\vec{q})} T_{L;qk}, \quad (107)$$

where we have written the quantities in matrix form, since the spectator momenta are now discrete, e.g.,  $B_{pk} = B(\vec{p}, \vec{k})$ . We stress again that there is an implicit dependence of all quantities on the overall energy  $E$ . In addition, the sum over  $\vec{q}$  has to be cut off, and in Refs. (23, 24) this is done with a hard cutoff  $|\vec{q}| < \Lambda$ . Then Eq. (107) is a matrix equation for  $T_L$  that can be inverted. Poles in  $\mathcal{M}_{3L}$  occur when  $T_L$  has a divergent eigenvalue, which leads to the quantization condition

$$\det(T_L^{-1}) = 0. \quad (108)$$

This can be further reduced by projecting onto irreps of the cubic group (23, 24, 56), but the unreduced form will be sufficient here.

The derivation is structurally similar to that given in the NREFT approach, with the LECs being replaced here by the unknown functions  $C$ ,  $\lambda$  and  $f$ . What differs is that, whereas in the NREFT approach loops involve only three particles, here, in any given relativistic theory, there are loops involving any (odd) number of particles. The claim is that the decomposition used above picks out all the three-particle loops that contain poles, because it is these loops that lead to the imaginary parts needed to satisfy unitarity. These loops must be summed when in finite volume, while the other loops (contained inside  $C$ ,  $\lambda$  etc.) can be kept in infinite volume. As for the two-particle quantization condition, this argument is very plausible, but does not constitute in our view a complete derivation. Thus we think that it is important to demonstrate the equivalence of Eq. (108) to the results of the RFT approach in the limit of including only the  $s$ -wave dimer, as we do in the following.

**3.2.3. Relation to RFT approach.** We begin by rewriting the FVU quantization condition. Defining  $\omega$  and  $D_L$  as diagonal matrices as in the RFT derivation, we can solve Eq. (107) to find

$$T_L = \frac{1}{1 + B \frac{1}{2\omega L^3 D_L}} B = 2\omega L^3 D_L \frac{1}{B + 2\omega L^3 D_L} B. \quad (109)$$

The quantization condition (108) can thus be rewritten as

$$\det(B + 2\omega L^3 D_L) = 0. \quad (110)$$

We next note that

$$B = -v_{\text{on}} G_s v_{\text{on}} (2\omega L^3) + C', \quad C' - C = v_{\text{on}} G_s v_{\text{on}} (2\omega L^3) - B_0, \quad (111)$$

<sup>25</sup>It is possible to change the definition of  $B_0$  away from the pole, leading to changes in the definition of  $C$ . Here we show the form from Ref. (57). Somewhat different choices are made in Refs. (23, 24).



with  $G_s$  the  $s$ -wave part of  $G$ , Eq. (38). The key point here is that the two terms in  $C' - C$  have the same residue at the OPE pole, so that the difference cancels the pole and is smooth.<sup>26</sup> We also need the result from Eqs. (103) and (104) that

$$D_L = -v_{\text{on}} (\mathcal{K}_{2,s}^{-1} + F_s) v_{\text{on}}, \quad (112)$$

where  $F_s$  is the matrix form of  $F_{2s}$  [see Eq. (36)]. Putting this all together, and using the smoothness of  $v_{\text{on}}$ , the FVU quantization condition becomes

$$\det \left[ \mathcal{K}_{2,s}^{-1} + F_s + G_s - \tilde{C} (2\omega L^3)^{-1} \right] = 0, \quad \tilde{C} = v_{\text{on}}^{-1} C' v_{\text{on}}^{-1}. \quad (113)$$

Aside from one technical point, to be discussed shortly, this is an exact rewriting of the result of Ref. (23). This new result looks very similar to the form of the NREFT quantization condition given in Eq. (87), with  $\tilde{C}$  here playing the role of  $2mL^3\bar{H}$ . This emphasizes again the close connection between the two approaches, although of course here the result here is not restricted to the NR regime.

The technical point just alluded to concerns the difference between the cutoff schemes in the RFT and FVU approaches: the former using the smooth cutoff function  $H(\vec{k})$ , the latter a hard cutoff  $\Lambda$ .<sup>27</sup> Thus, for example,  $F_s$  from Eq. (36) includes  $H(\vec{k})$ , whereas  $D_L$  does not. Similarly there is a contribution to  $\mathcal{K}_{2,s}$  proportional to  $1 - H(\vec{k})$  that turns on near the cutoff. This implies that Eq. (112) breaks down for  $|\vec{k}| \sim m$ , and thus that Eq. (113) is not strictly a valid rewriting of the FVU quantization condition. We view this, however, as a technical, and not a fundamental, issue. The differences between cutoffs occur for spectator momenta such that  $E_{2,k}^{*2} \lesssim 0$ . In this regime, the three-particle threshold lies far away (it opens up at  $E_{2,k}^{*2} = 4m^2$ ). Thus the contributions to the sum over  $\vec{k}$  with  $E_{2,k}^{*2} \lesssim 0$  lead only to exponentially-suppressed volume effects, and we expect that varying the cutoff in this regime can be compensated by changes to infinite-volume quantities, namely the functions  $C$  and  $\mathcal{K}_{\text{df},3}$ . This is exactly what happens in NREFT, but in that case in a way that is simple to calculate. Here the cutoff dependence of  $C$  and  $\mathcal{K}_{\text{df},3}$  will not be simple. In light of these considerations, we will proceed using Eq. (113) as written.

Returning to the algebraic relation between the quantization conditions, we begin from the form of the RFT quantization condition, Eq. (89), that looks most similar to the FVU result, Eq. (113). As in the NREFT case, this similarity is superficial, because  $\bar{H}^R$  in the former equation and  $\tilde{C}/(2\omega L^3)$  here have very different properties. However, if we assume that  $\mathcal{K}_{\text{df},3,s}$  is isotropic,  $\mathcal{K}_{\text{df},3,s} = |1\rangle \mathcal{K}_{\text{df},3}^{\text{iso}} \langle 1|$ , then, by essentially the same algebraic steps as earlier, we can show that the two quantization conditions agree if

$$\tilde{C} = \left[ 1 + (\mathcal{K}_{2,s}^{-1} + I_s) \frac{\mathcal{K}_{\text{df},3,s}}{9L^3} \frac{1}{2\omega} \right]^{-1} (\mathcal{K}_{2,s}^{-1} + I_s) \frac{\mathcal{K}_{\text{df},3,s}}{9} (\mathcal{K}_{2,s}^{-1} + I_s). \quad (114)$$

Here the relativistic generalization of the integral  $I_s^{\text{NR}}$  is

$$I_{s,pk} = \delta_{pk} \text{PV} \int_{\vec{a}} \frac{H(\vec{a})}{2\omega_a ([P - k - a]^2 - m^2)}, \quad (115)$$

where a specific choice for the regulator has been made. Unlike in the NR regime, this integral does depend on  $\vec{k}$ . Using the definition of  $\tilde{C}$ , we can manipulate Eq. (114) into an equation for  $C'$ :

$$C' = v_{\text{on}} (\mathcal{K}_{2s}^{-1} + I_s) |1\rangle \frac{1}{1 + \mathcal{K}_{\text{df},3}^{\text{iso}} \langle 1| (2\omega)^{-1} (\mathcal{K}_{2,s}^{-1} + I_s) |1\rangle / (9L^3)} \frac{\mathcal{K}_{\text{df},3}^{\text{iso}} \langle 1| (\mathcal{K}_{2,s}^{-1} + I_s) v_{\text{on}}}{9}. \quad (116)$$

This provides an explicit relation between the quantization conditions in the limit of an isotropic  $\mathcal{K}_{\text{df},3,s}$ . Note that

$$\frac{\langle 1| (2\omega)^{-1} (\mathcal{K}_{2,s}^{-1} + I_s) |1\rangle}{L^3} = \int_{\vec{k}} \frac{\mathcal{K}_{2,s}(\vec{k})^{-1} + I_s(\vec{k})}{2\omega_k} + \mathcal{O}([\Lambda L]^{-1}), \quad (117)$$

so the right-hand side of Eq. (116) is volume independent up to cutoff effects.

The most important lesson from Eq. (116) is that, if  $\mathcal{K}_{\text{df},3,s}$  is isotropic, then the function  $C'$  cannot be. The main reason for this is the presence of the vertex factors  $v_{\text{on}}$  in Eq. (116). Recall that  $v_{\text{on}}$  is a diagonal matrix with entries

$$\lambda(E_{2,k}^{*2}) f(Q_k^2), \quad Q_k^2 = E_{2,k}^{*2} - 4m^2. \quad (118)$$

Thus it has a significant dependence on  $\vec{k}$ , with  $f$  increasing as  $|\vec{k}|$  becomes large and  $Q_k^2$  becomes negative with a large magnitude. Additional dependence on  $\vec{k}$  enters through both  $\mathcal{K}_{2,s}$  and  $I_s$ . This means that the vector

$$v_{\text{on}} (\mathcal{K}_{2,s}^{-1} + I_s) |1\rangle \quad (119)$$

<sup>26</sup>Away from the pole, the two terms on the right-hand side of  $C' - C$  differ both because  $G_s$  contains cutoff functions  $H(k)$  while  $B_0$  does not, but also because the vertices in  $B_0$  are evaluated off shell.

<sup>27</sup>In this regard, we note that the vertex functions in the FVU approach do not provide damping factors in the sums over spectator momenta, as can be seen for example by the appearance of  $v_{\text{on}}^{-1}$  in  $\tilde{C}$ .

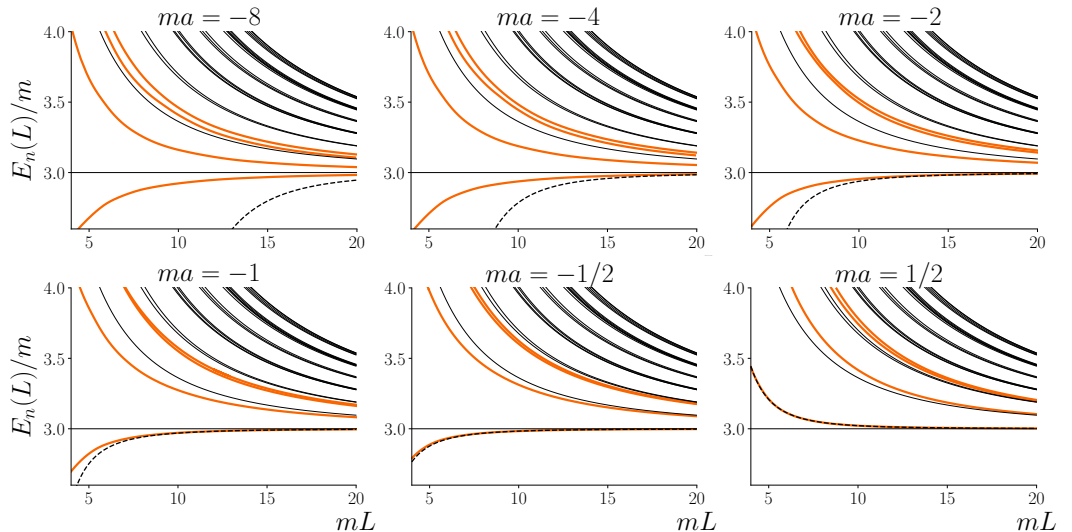


**Figure 5**

Spectrum of three-particle states evaluated using the RFT formalism in the isotropic approximation, for various choices of the scattering length,  $a$ , and vanishing three-body interaction,  $\mathcal{K}_{\text{df},3}^{\text{iso}} = 0$ . The thick orange curves show the interacting levels and the thin black lines show the corresponding energies of three non-interacting particles (i.e. the spectrum when  $a = 0$ ). In each plot, the dashed curve shows the  $1/L$  expansion for the threshold state, Eq. (62), which is expected to work well when  $a/L \ll 1$ .

appearing on both ends of the expression for  $C'$  is far from isotropic once one leaves the NR regime. We stress that this difference occurs not just near the cutoff, but rather over the entire range of relativistic spectator momenta.

We do not think this conclusion is fundamentally surprising, since we do not expect either  $\mathcal{K}_{\text{df},3}$  or  $C'$  to be close to isotropic once one leaves the NR regime. Indeed, as shown in Refs. (35, 37), one can systematically expand  $\mathcal{K}_{\text{df},3}$  about threshold, and only the leading two terms are isotropic. Presumably the same holds for  $C'$ . Once in the relativistic domain one needs the whole tower of higher-order terms, which are not isotropic (and also bring in higher-order dimers).

**3.2.4. Summary.** The FVU method provides a direct and relatively simple approach to obtain the three-particle quantization condition that is not restricted to the NR regime. It follows steps that are, roughly speaking, the relativized version of those used in the NREFT derivation. The simplicity compared to the RFT approach is partly due to keeping only a single dimer, but mainly because unitarity is used to determine which finite-volume momentum sums have singular summands, rather than a diagrammatic analysis. Another advantage of the FVU approach is that it is expected to work also in the presence of subchannel resonances.

As noted above, we find the arguments for this approach very plausible, but are not convinced that it constitutes a complete derivation. Thus we think that it is important to show that it is equivalent to the result of the RFT approach. We have taken the first steps in this direction above, showing algebraic equivalence in the particular case of an isotropic  $\mathcal{K}_{\text{df},3,s}$ . Extending this analysis to more general forms for  $\mathcal{K}_{\text{df},3}$  and to include higher-order dimers is an important future challenge.

An important issue in this regard is whether the parametrization of  $\mathcal{M}_3$  given in Ref. (57) is completely general. One way of checking this would be to make a detailed comparison with the representation of  $\mathcal{M}_3$  in terms of  $\mathcal{K}_{\text{df},3}$  that is a byproduct of the RFT approach (sketched in Sec. 2.2.4 above) (18). Since this representation follows from an all-orders diagrammatic approach, it must be unitary, and indeed this can be shown explicitly (34).

## 4. NUMERICAL IMPLEMENTATIONS

In this section we give a brief summary of numerical results that have been calculated using each of the three formalisms presented above. In all cases, the results were determined by taking a model or ansatz for the infinite-volume interactions and then determining the corresponding finite-volume energy levels. We view these results as a proof of principle that, for all three formalisms, the mapping between finite-volume energies and infinite-volume scattering observables is feasible. A dedicated study in which only LQCD inputs are used to extract the three-body scattering amplitude has yet to be implemented, although Ref. (24) already made first steps in this direction.

Beginning with the RFT formalism described in Sec. 2.2, here we present two numerical results that are described in greater detail in Ref. (37). In both calculations, the numerical evaluation was performed using the isotropic approximation, outlined in Sec. 2.3. We additionally considered systems for which the two-to-two scattering amplitude is well-described by the leading-order effective-range expansion, and thus depends only on the scattering length,  $a$ .

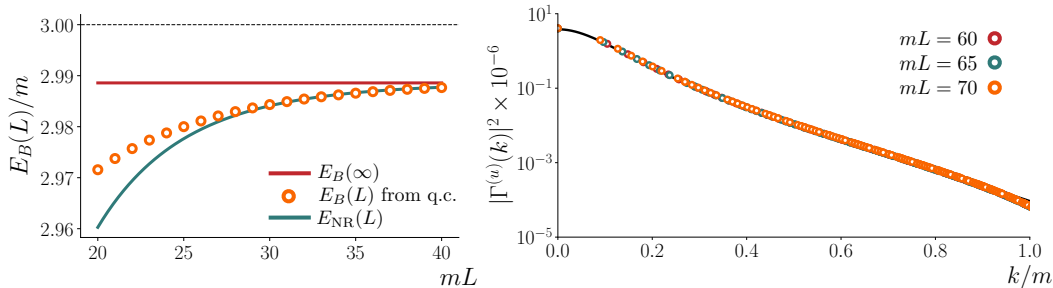


**Figure 6**

Finite-volume bound-state energy (left) and the corresponding infinite-volume wave function (right). In the left panel we show the infinite-volume bound-state mass (horizontal red line) together with the leading-order non-relativistic prediction (green curve) and the result of numerically solving the RFT quantization condition (orange points). The asymptotic prediction agrees well with the numerical solution for  $\kappa L > 3$ , but deviates for smaller volumes, as expected. The right panel shows the result for the residue of  $\mathcal{M}_3$  at the bound-state pole, obtained by solving the integral equations relating  $\mathcal{K}_{\text{df},3}$  to  $\mathcal{M}_3$ . We use a very large effective volume as a tool for numerically solving the infinite-volume equations and the consistency of the various data points indicates that we have reached the infinite-volume limit to high precision. The solid black curve is an analytic prediction (not a fit to the data) given in Ref. (47).

For our first application, we suppose that the local three-body interaction is negligible and set  $\mathcal{K}_{\text{df},3}^{\text{iso}} = 0$ . Within this set-up, each choice of scattering length gives a prediction for the three-particle energies  $E_n(L)$ , as shown in **Figure 5**. These curves serve as a benchmark since, in future LQCD calculations, only by measuring deviations from the  $\mathcal{K}_{\text{df},3} = 0$  predictions can one obtain information about three-body interactions.

In the second numerical example from Ref. (37), we work close to the unitary limit  $1/(ma) = -10^{-4}$ , corresponding to a two-particle interaction that almost, but not quite, leads to a bound dimer. In this limit, we find that, still working in the isotropic approximation, we can tune  $\mathcal{K}_{\text{df},3}^{\text{iso}}$  so that the infinite-volume system develops an Efimov-like bound state (45). In our example, the bound state energy is  $E_B \approx 2.99m$ , corresponding to a binding momentum of  $\kappa \approx 0.1m$ . The quantization condition then determines the volume dependence of this state, with results that are compared with the prediction of Ref. (46), Eq. (64), in the left panel of **Figure 6**. We find good agreement for sufficiently large  $L$ , with the single parameter determined to be  $|A|^2 \approx 0.95$ . This is in the expected range of values, i.e. close to unity. We expect, and find, that the curve deviates from the asymptotic form once  $\kappa L < 3$ , because neglected  $1/(\kappa L)$  corrections then become important. A key point, however, is that the quantization condition itself incorporates all terms suppressed by any power or any exponent of  $\kappa L$ . Its validity requires only that  $mL$  is sufficiently large. Thus one could, in this simple model, extract a value for  $\mathcal{K}_{\text{df},3}^{\text{iso}}$  from the spectrum for  $mL \approx 5$  (where typical LQCD calculations are done), in a regime where the asymptotic formula, Eq. (64), completely fails.

The right panel of **Figure 6** shows a further test of the RFT formalism. Here we implemented our  $\mathcal{K}_{\text{df},3} \Rightarrow \mathcal{M}_3$  relation (described in Sec. 2.2.4) to obtain the residue of  $\mathcal{M}_3$  at the bound-state pole. The resulting, numerically-determined residue is compared to the known analytic prediction in the plot. This prediction is derived in Ref. (47) using NRQM, and, given the result for  $|A|^2$  from the fit to the spectrum, is parameter-free. The good agreement over seven orders of magnitude shows that this simple model of interactions captures the physics of the Efimov effect over a wide range of scales.

We next describe an example of the numerical results obtained using the NREFT approach, as presented in Ref. (56). The setup is quite similar to that just described for the RFT results, with the two-particle interactions described by an  $s$ -wave scattering length, and a single isotropic three-body coupling constant. The total momentum is  $\vec{P} = 0$ , and only the  $A_1^+$  irrep is considered. The scattering length is chosen so that there is a bound dimer with NR energy,  $E_{\text{NR}} = -1/(ma^2)$ , and  $H_0$  is chosen so that there is a deeply bound trimer with  $E_{\text{NR}} = -10/(ma^2)$ . It turns out that, with these parameters, there is, in infinite volume, a second trimer, with  $E_{\text{NR}} = -1.016/(ma^2)$ , consisting of a loosely bound dimer and particle. In finite volume, one then expects a plethora of states: the deeply bound trimer with (asymptotically predicted) volume dependence, the second trimer with a different volume dependence, a spectrum of states lying close to the energies of a noninteracting dimer and particle, and, finally, states that lie near the energies of three free particles. An example of the resulting spectrum is shown in **Figure 7**, with only the non-bound-states shown. The expected states are seen, but with a number of avoided level crossings making the interpretation nontrivial. The overall conclusion is that this rather complicated physical situation is successfully encoded into the NREFT quantization condition.

Finally, we describe results from a recent numerical study of the FVU approach (24). In this study the authors were motivated to make contact with a physical system by considering finite-volume  $\pi^+\pi^+$  as well as  $\pi^+\pi^+\pi^+$  states. They work in the isospin-symmetric limit, so these two sectors are not connected. The  $\pi^+\pi^+ \rightarrow \pi^+\pi^+$  scattering amplitude, needed as an input

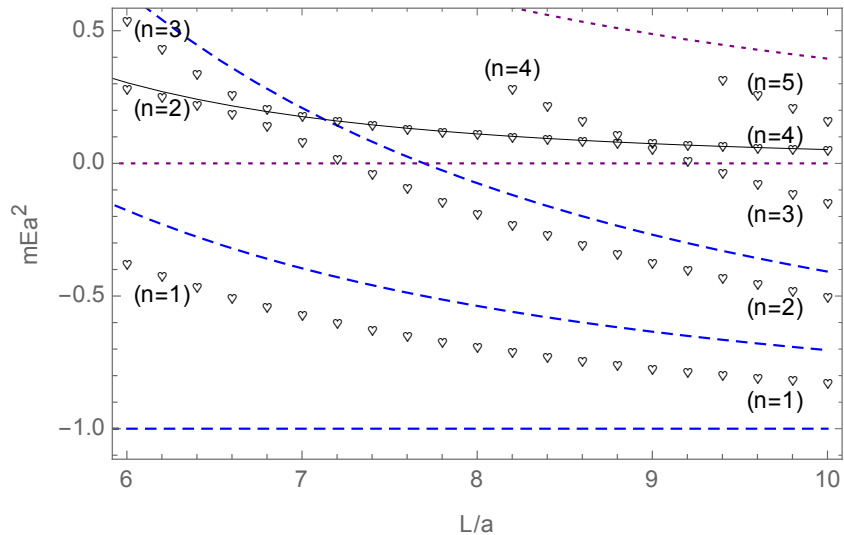


**Figure 7**

Example of three-particle energy levels obtained using the NREFT quantization condition in Ref. (56). Here  $E$  is the NR energy, called  $E_{\text{NR}}$  elsewhere in this review. The triangles show the results of solving the quantization condition for the parameters described in the text. Only the states above the bound dimer-particle threshold at  $E_{\text{NR}} = -1/(ma^2)$  are shown (so the two bound trimer states lie below the bottom of the plot and are not visible). The dashed blue lines show the energies of noninteracting dimer-particle states with varying back-to-back momenta. The purple dotted curves show the free three-particle states. The solid black line is the prediction of the threshold expansion, Eq. (62), keeping terms only up to  $\mathcal{O}(1/L^5)$ . We observe that dimer-particle interactions push the energies up in finite volume, as shown by the lowest two [ $(n=1)$  and  $(n=2)$ ] levels shown. The third level shown, however, changes its nature as  $L/a$  decreases: starting as a dimer-particle state, converting to a three-particle threshold state at  $L/a \sim 9$ , and then converting back to a different particle-dimer state at  $L/a \sim 6.5$ .

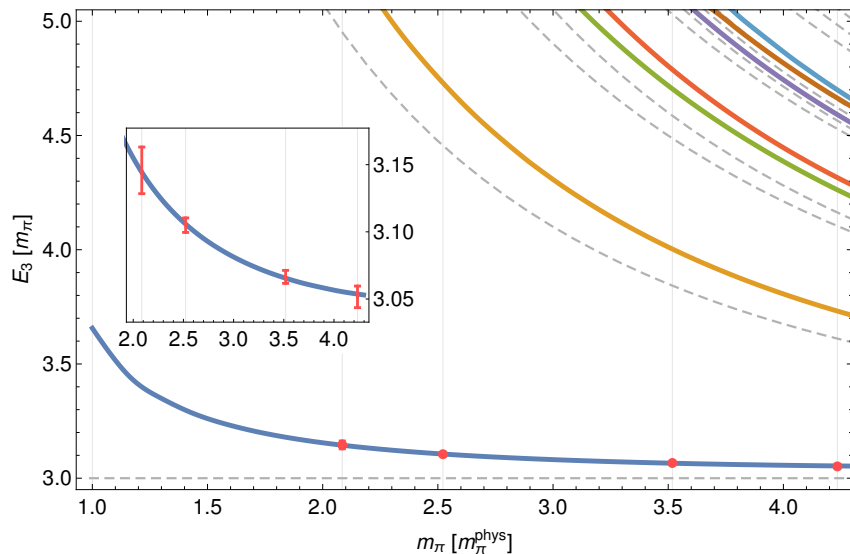


**Figure 8**

Three-pion energy levels (solid lines, various colors) presented in Ref. (24). The curves are based on two-to-two interactions determined from chiral perturbation theory combined with the inverse amplitude method. As in **Figure 5**, the three-body interaction term,  $C$ , is set to zero. In contrast to previous plots, in this case the interactions and the values of  $m_\pi L$  are varying simultaneously, by changing the physical value of  $m_\pi$  while keeping the box size fixed at  $L = 2.5$  fm. Only states in the  $A_1^+$  irrep are shown, and the dashed lines show the noninteracting three-particle levels. The inset zooms in on the fit that is used to constrain the three-particle interaction. We caution that the lowest plotted values of  $m_\pi$  correspond to  $m_\pi L \approx 1.8$ , for which the neglected, exponentially-suppressed terms may be significant.

to the quantization condition, was modeled by combining chiral perturbation theory amplitudes with the so-called inverse amplitude method. The resulting functional form also encodes pion-mass dependence, allowing  $m_\pi$  to be varied from its physical value to a value around four times larger. In the energy range considered the approximation of keeping only  $s$ -wave dimers is expected to be very good.

This set-up enabled the authors to change  $m_\pi L$  while holding the box size fixed at  $L = 2.5$  fm, with the resulting finite-volume energies varying due to the change in the effective box size (measured in units of  $m_\pi$ ) as well as due to modifications in the interactions of the theory. **Figure 8**

shows the the resulting spectrum of  $\pi^+\pi^+\pi^+$  states. For the lowest level (the threshold state) the energies can be compared to those previously determined by the NPLQCD collaboration in a numerical LQCD calculation (58, 59), allowing the three-body coupling  $C$  to be constrained. Using the (non-isotropic) form  $C(\vec{p}, \vec{q}) = c \delta^3(\vec{p} - \vec{q})$ , the result is consistent with zero,  $c = (0.2 \pm 1.5) \times 10^{-10}$ .

### SUMMARY POINTS

1. A method for determining predictions from lattice QCD (LQCD) for the properties of resonances that have decay channels into three or more particles is urgently needed. This will allow LQCD to address the nature of many of the higher-lying resonances, in particular the recently observed  $X$ ,  $Y$  and  $Z$  states.
2. To address this problem one requires a quantization condition that relates the finite-volume spectrum of QCD, which can be obtained directly in LQCD calculations, to the infinite-volume scattering amplitudes that encode resonance properties. The two-particle quantization condition is known and widely used; this review focuses on progress towards the three-particle quantization condition.
3. Three approaches have been used: one that is general and relativistic (RFT approach), and also leads to a very complicated derivation; a second based in NREFT that leads to a much simpler derivation; and a third that implements the constraints of unitarity in the finite volume (FVU approach), which also leads to a simpler derivation than the RFT approach but is nevertheless relativistic. The latter two approaches have only been formulated to date for  $s$ -wave dimer interactions.
4. All three approaches lead to a two-step relation between the finite-volume spectrum and infinite-volume scattering amplitudes, involving intermediate, cut-off dependent, unphysical infinite-volume quantities.
5. The three approaches can be shown to be equivalent in certain regimes.
6. All three approaches have been successfully implemented numerically in model calculations using the simplest approximations for interactions.

### FUTURE ISSUES

The development of the three-particle quantization condition has reached a pivotal stage. The groundwork has been laid, but many technical issues must be addressed for the methodology to be applicable to most resonances of phenomenological interest. Overall, we think that resolving these issues will be more straightforward than the work that has been done so far, and thus we are optimistic about the future applicability of the methodology. We list here those issues that we consider most pressing.

1. For all approaches, the formalism needs to be generalized to incorporate nonidentical particles and particles with nonzero spin.
2. The NREFT and FVU approaches need to be extended to include dimers beyond  $s$ -waves and moving frames, and to include the possibility of  $2 \leftrightarrow 3$  transitions.
3. The NREFT approach needs to be “relativized” in order to be applicable to results from LQCD.
4. In the RFT approach, the second step of connecting  $\mathcal{K}_{\text{df},3}$  to  $\mathcal{M}_3$  must be implemented above threshold. This work is further advanced in the NREFT and FVU approaches.
5. A technical issue in the RFT approach as presently formulated is the need to use a relatively low cutoff (so that two-particle invariant masses are kept positive, i.e.  $E_{2,k}^{*2} \geq 0$ ). Extending the formalism to allow a higher cutoff (concomitant with that used in the other approaches) should be investigated. This is also related to an issue that we have not had space to discuss here, namely whether the presence of the left-hand cut in the two-particle amplitude (which opens up at  $E_{2,k}^{*2} = 0$ ) can lead to difficulties for the formalisms.
6. Practical parametrizations of the three-particle interaction terms— $\mathcal{K}_{\text{df},3}$ ,  $H(\Lambda)$  and  $C$ —must be developed that are based on phenomenological input and are flexible enough to describe resonances encountered in the strong interactions.
7. The numerical implementations must be extended to include  $2 \leftrightarrow 3$  transitions. This is needed, for example, to study the Roper resonance.
8. The relation between the approaches must be studied when higher-spin dimers and more complicated three-particle interactions are included.
9. Ultimately, the extension to four or more particles must be considered. This has been worked out so far only for the energy of the threshold state in NRQM (38) and for the volume dependence of an  $N$ -body NR bound state (60).

## DISCLOSURE STATEMENT

The authors are not aware of any affiliations, memberships, funding, or financial holdings that might be perceived as affecting the objectivity of this review.

## ACKNOWLEDGMENTS

We are grateful to Michael Döring, Hans-Werner Hammer, Maxim Mai, and Akaki Rusetsky for helpful discussions and correspondence, and to them, Jin-Yi Pang and J. Wu for giving us permission to use plots from their work. The work of SRS is supported in part by the United States Department of Energy grant No. de-sc0011637.

## LITERATURE CITED

1. Gross DJ, Wilczek F. *Phys. Rev. Lett.* 30:1343 (1973).
2. Politzer HD. *Phys. Rev. Lett.* 30:1346 (1973)
3. Fritzsche H, Gell-Mann M, Leutwyler H. *Phys. Lett. B* 47:365 (1973)
4. Jaffe RL. *Phys. Rev. D* 15:267 (1977); *ibid* 15:281 (1977)
5. Aaij R, et al. (LHCb Collab.) *Phys. Lett. B* 772:265 (2017)
6. Karliner M, J. L. Rosner JL, Skwarnicki T. *Ann. Rev. Nucl. Part. Sci.* 68:17 (2018)
7. Tanabashi M, et al. (Part. Data Group) *Phys. Rev. D* 98:030001 (2018)
8. Aoki S, et al. (FLAG Collab.) *Eur. Phys. J. C* 77:112 (2017)
9. Lüscher M. *Commun. Math. Phys.* 104:177 (1986)
10. Lüscher M. *Commun. Math. Phys.* 105:153 (1986)
11. Lüscher M. *Nucl. Phys. B* 354:531 (1991)
12. Briceño RA, Dudek JJ, Young RD. *Rev. Mod. Phys.* 90:025001 (2018)
13. Dudek JJ, et al. (Hadron Spectrum Collab.) *Phys. Rev. D* 88:094505 (2013)
14. Bulava J, Fahy B, Hörz B, Juge K-J, Morningstar C, Wong CH. *Nucl. Phys. B* 910:842 (2016)
15. Polejaeva K, Rusetsky A. *Eur. Phys. J. A* 48:67 (2012)
16. Briceño RA, Davoudi Z. *Phys. Rev. D* 87:094507 (2013)
17. Hansen MT, Sharpe SR. *Phys. Rev. D* 90:116003 (2014)
18. Hansen MT, Sharpe SR. *Phys. Rev. D* 92:114509 (2015)
19. Briceño RA, Hansen MT, Sharpe SR. *Phys. Rev. D* 95:074510 (2017)
20. Briceño RA, Hansen MT, Sharpe SR. *Phys. Rev. D* to appear (2018)
21. Hammer H-W, Pang J-Y, Rusetsky A. *JHEP* 1709:109 (2017)
22. Hammer H-W, Pang J-Y, Rusetsky A. *JHEP* 1710:115 (2017)
23. Mai M, Döring M. *Eur. Phys. J. A* 53:240 (2017)
24. Mai M, Döring M. arXiv:1807.04746 [hep-lat].
25. Aoki S et al. (HALQCD Collab.) *PTEP* 2012: 01A105 (2012) and *Prog. Part. Nucl. Phys.* 66:687 (2011)
26. Gongyo S et al. (HALQCD Collab.) *Phys. Rev. Lett.* 120:212001 (2018)
27. Doi T et al. (HALQCD Collab.) *Prog. Theor. Phys.* 127:723 (2012)
28. Lee D, Epelbaum E, Krebs H, Meißner UG. *PoS CD* 09:027 (2009)
29. Elhatisari S et al. *Phys. Rev. Lett.* 119:222505 (2017)
30. Guo P, Döring M, Szczepaniak AP. *Phys. Rev. D* 98:094502 (2018)
31. Lüscher M, Wolff U. *Nucl. Phys. B* 339:222 (1990).
32. Huang K, Yang CN. *Phys. Rev.* 105:767 (1957).
33. Kim CH, Sachrajda CT, Sharpe SR. *Nucl. Phys. B* 727:218 (2005)
34. Briceño RA, Hansen MT, Sharpe SR, Szczepaniak A. Work in progress (2019)
35. Blanton TD, Briceño RA, Hansen MT, Romero-López F, Sharpe SR. arXiv:1810.06634 [hep-lat]
36. Blanton TD, Romero-López F, Sharpe SR. Work in progress (2019)
37. Briceño RA, Hansen MT, Sharpe SR. *Phys. Rev. D* 98:014506 (2018)
38. Beane SR, Detmold W, Savage MJ. *Phys. Rev. D* 76:074507 (2007)
39. Tan S. *Phys. Rev. A* 78:013636 (2008)
40. Detmold W, Savage MJ. *Phys. Rev. D* 77:057502 (2008)
41. Hansen MT, Sharpe SR. *Phys. Rev. D* 93:096006 (2016) [Erratum: *ibid* 96:039901 (2017)]
42. Hansen MT, Sharpe SR. *Phys. Rev. D* 93:014506 (2016)
43. Sharpe SR. *Phys. Rev. D* 96:054515 (2017) [Erratum: *ibid* 98:099901 (2018)]
44. Romero-López F, Rusetsky A, Urbach C. *Eur. Phys. J. C* 78:846 (2018)
45. Efimov V. *Phys. Lett. B* 33:563 (1970)
46. Meißner UG, Ríos G, Rusetsky A. *Phys. Rev. Lett.* 114:091602 (2015) [Erratum: *ibid* 117:069902 (2016)]
47. Hansen MT, Sharpe SR. *Phys. Rev. D* 95: 034501 (2017)
48. Kreuzer S, Hammer H-W. *Phys. Lett. B* 673:260 (2009)
49. Kreuzer S, Hammer H-W. *Eur. Phys. J. A* 43:229 (2010)
50. Kreuzer S, Hammer H-W. *Phys. Lett. B* 694:424 (2011)
51. Chen J-W, Rupak G, Savage MJ. *Nucl. Phys. A* 653:386 (1999)
52. Hammer H-W, Rusetsky A. Private communication.
53. Bedaque PF, van Kolck U. *Ann. Rev. Nucl. Part. Sci.* 52:339 (2002)
54. Kaplan DB, Savage MJ, Wise MB. *Phys. Lett. B* 424:390 (1998)
55. Phillips DR, Beane SR, Birse MC. *J. Phys. A* 32:3397 (1999)
56. Döring M, Hammer H-W, Mai M, Pang J-Y, Rusetsky A, Wu J. *Phys. Rev. D* 97:114508 (2018)
57. Mai M, Hu B, Döring M, Pilloni A, Szczepaniak A. *Eur. Phys. J. A* 53:177 (2017)
58. Beane SR, Detmold W, Luu TC, Orginos K, Savage MJ, Torok A. *Phys. Rev. Lett.* 100:082004 (2008)

59. Detmold W, Savage MJ, Torok A, Beane SR, Luu TC, Orginos K, Parreno A. *Phys. Rev. D* 78:14507 (2008)
60. König S, Lee D. *Phys. Lett. B* 779:9 (2018)